

Contrasting forms of cocaine-evoked plasticity control components of relapse

Vincent Pascoli^{1*}, Jean Terrier^{1*}, Julie Espallergues^{2,3,4}, Emmanuel Valjent^{2,3,4}, Eoin Cornelius O'Connor¹ & Christian Lüscher^{1,5}

Nucleus accumbens neurons serve to integrate information from cortical and limbic regions to direct behaviour. Addictive drugs are proposed to hijack this system, enabling drug-associated cues to trigger relapse to drug seeking. However, the connections affected and proof of causality remain to be established. Here we use a mouse model of delayed cue-associated cocaine seeking with *ex vivo* electrophysiology in optogenetically delineated circuits. We find that seeking correlates with rectifying AMPA (α -amino-3-hydroxy-5-methyl-4-isoxazole propionic acid) receptor transmission and a reduced AMPA/NMDA (*N*-methyl-D-aspartate) ratio at medial prefrontal cortex (mPFC) to nucleus accumbens shell D1-receptor medium-sized spiny neurons (D1R-MSNs). In contrast, the AMPA/NMDA ratio increases at ventral hippocampus to D1R-MSNs. Optogenetic reversal of cocaine-evoked plasticity at both inputs abolishes seeking, whereas selective reversal at mPFC or ventral hippocampus synapses impairs response discrimination or reduces response vigour during seeking, respectively. Taken together, we describe how information integration in the nucleus accumbens is commandeered by cocaine at discrete synapses to allow relapse. Our approach holds promise for identifying synaptic causalities in other behavioural disorders.

The nucleus accumbens (NAc) is a point of convergence for excitatory afferents arising from limbic and cortical regions, including the basolateral amygdala (BLA), ventral hippocampus (vHipp) and the mPFC. From pharmacology, lesion and imaging experiments, each of these regions is thought to signal distinct information to the NAc during reward-related situations. Specifically, the BLA signals emotional valence, the vHipp provides contextual relevance, whereas the mPFC provides action–outcome information^{1,2}. NAc neurons select and integrate information from these diffuse regions and signal to the basal ganglia motor system to guide appropriate behaviours, such as foraging in response to feeding relevant signals^{3,4}. This neural circuitry is also involved in core features of drug addiction, such as craving and relapse in response to drug-associated cues after withdrawal periods^{5,6}. Understanding how this circuitry is ‘hijacked’ after drug experience and how drug-evoked alterations are causally related to drug-adaptive behaviours, such as relapse, is fundamental to defining the pathophysiology of addiction.

The task of information processing and output in the NAc falls to MSNs, representing 95% of NAc neurons and broadly divisible into two equally sized classes according to the dopamine receptors expressed⁷. Both NAc D1 receptor (D1R)-MSN and D2 receptor (D2R)-MSN subtypes receive excitatory afferents from the BLA, vHipp and mPFC^{4,8}, but differ in their projection targets^{3,9}. Owing to the arrangement of synapses on MSN spines, excitatory transmission arriving onto the spine head is subject to strong modulation by dopamine from the ventral tegmental area arriving at the spine neck¹⁰. Indeed, dopamine gates excitatory transmission, allowing synaptic adaptations and modulation of reward-related behaviours^{11–13}. Accumbal dopamine transients induced by addictive drugs are probably key for inducing circuit adaptations that divert behaviour towards compulsive drug seeking and heighten the risk of relapse after prolonged withdrawal^{14,15}. Relapse is associated with exposure to drug cues, it is context dependent and requires knowledge of what actions result in drug delivery⁵. Therefore, this behaviour is likely underpinned by a memory trace, formed in the reward circuitry

during drug use^{16,17}. However, the nature of this trace and the causal implications remain elusive.

Much literature has described induction requirements and expression mechanisms for drug-evoked plasticity at excitatory synapses, including those of the NAc¹⁷. The time after the last drug exposure is important, as the expression of some forms of plasticity can take days or weeks^{18,19}. Therefore, establishing a causal link between drug-evoked plasticity and drug-adaptive behaviours has been difficult. Pharmacological manipulation of AMPA receptors (AMPA receptors) implicates NAc glutamatergic transmission in cue-associated cocaine seeking^{20,21}, but many questions remain. Do different excitatory inputs change in the same way onto D1R- and D2R-MSNs after withdrawal from cocaine self-administration? Could drug-evoked alterations at specific inputs be causally linked to specific components of drug-adaptive behaviours, such as relapse? Here we use cell-type-specific reporter lines and optogenetics to address these questions, taking an approach that may also be applied in other behavioural disorders to establish synaptic causalities (Extended Data Fig. 1).

Cocaine-evoked plasticity at D1R-MSNs

To characterize drug-evoked plasticity in identified NAc MSNs at a time point when relapse can be observed, bacterial artificial chromosome (BAC) transgenic mice expressing fluorescent proteins under the control of the D1R or D2R promoter were first trained to self-administer intravenous cocaine²². Control mice that received only intravenous saline infusions quickly stopped responding, whereas mice that self-administered cocaine learned to discriminate between the active and inactive levers and responded almost exclusively on the active lever at the end of the acquisition phase, confirming successful acquisition of cocaine self-administration (Fig. 1a, b).

Thirty days after the last self-administration session, whole-cell recordings were made *ex vivo* in identified NAc MSNs with excitatory postsynaptic currents (EPSCs) elicited by electrical stimulation to obtain a global overview of cocaine-evoked plasticity (Fig. 1c). The rectification

¹Department of Basic Neurosciences, Medical Faculty, University of Geneva, CH-1211 Geneva, Switzerland. ²INSERM, U661, Montpellier F-34094, France. ³CNRS, UMR-5203, Institut de Génétique Fonctionnelle, Montpellier F-34094, France. ⁴Universités de Montpellier 1 & 2, UMR-5203, Montpellier F-34094, France. ⁵Clinic of Neurology, Department of Clinical Neurosciences, Geneva University Hospital, CH-1211 Geneva, Switzerland.

*These authors contributed equally to this work.

index of AMPAR-EPSCs was increased selectively in D1R-MSNs from mice that self-administered cocaine, suggesting the presence of GluA2-lacking calcium-permeable AMPARs (CP-AMPA²³). The ratio of the amplitude of AMPAR- and NMDAR-EPSCs (*A/N* ratio) recorded in the same cells, which provides a measure of synaptic strength, was also increased only in D1R-MSNs from mice that self-administered cocaine (Fig. 1c). At first glance, it was surprising to observe these two forms of plasticity in the same neuron, because CP-AMPA²³ shows reduced conductance at +40 mV that would produce a decreased *A/N* ratio, if NMDA were unchanged. One potential explanation is that cocaine induced several contrasting forms of plasticity that segregate between different inputs onto the same D1R-MSNs. In support of this idea, a recent study reported an increased *A/N* ratio specifically at vHipp to NAc synapses after chronic non-contingent cocaine injections, without, however, resolving the MSN identity²⁴.

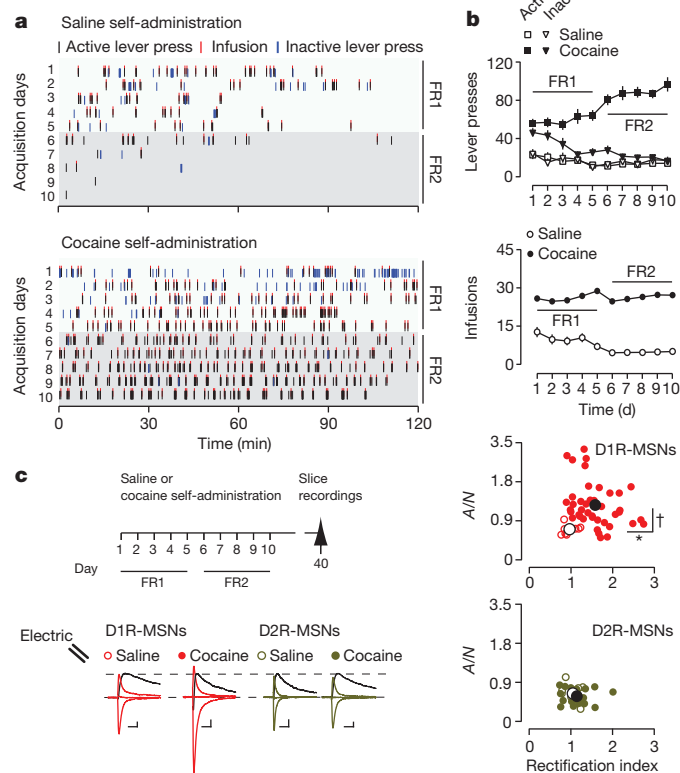


Figure 1 | Withdrawal from cocaine self-administration evokes cell-type-specific modifications of excitatory synapses in the NAc. **a**, Raster plot for infusions, active and inactive lever presses as a function of time during acquisition of self-administration for a mouse that self-administered saline (top) or cocaine (bottom). FR1, FR2, fixed-ratio one and two schedules. **b**, Mean total lever presses (top) and infusions (bottom) during the acquisition phase of saline ($n = 42$) or cocaine ($n = 164$) self-administration for all mice used in the study. **c**, Schematic of experiment (top). Sample traces of AMPAR-EPSCs at -70, 0 and +40 mV (coloured) and NMDAR-EPSCs at +40 mV (black) (bottom) and plots (right) of *A/N* ratio as a function of rectification index (small dots) for each D1R- ($n = 9/41$, saline/cocaine) or D2R-MSN ($n = 8/25$). Large open and filled dots represent group mean saline and cocaine data, respectively. Cocaine increased rectification index and *A/N* ratio in D1R-MSNs but not in D2R-MSNs (rectification index in D1R- and D2R-MSNs: effect of group (cocaine/saline), $F_{1,83} = 10.86$, $P < 0.01$; cell type \times group, $F_{1,83} = 6.08$, $P < 0.05$. Student's *t*-test for cocaine versus saline in D1R-MSNs, $t_{48} = 3.72$, $*P < 0.01$; in D2R-MSNs, $t_{31} = 0.80$, $P = 0.43$. *A/N* ratio in D1R- and D2R-MSNs: effect of group, $F_{1,83} = 5.91$, $P < 0.05$; cell type \times group, $F_{1,83} = 8.34$, $P < 0.01$. Student's *t*-test for cocaine versus saline in D1R-MSNs, $t_{48} = 3.25$, $\dagger P < 0.01$, in D2R-MSNs, $t_{31} = 0.62$, $P = 0.54$). Scale bars, 20 pA, 20 ms. Plots, means with s.e.m.

Cocaine-evoked plasticity at identified inputs

To explore the possibility that distinct afferents to the NAc undergo contrasting forms of plasticity after cocaine self-administration, the optogenetic effector channelrhodopsin tagged with enhanced yellow fluorescent protein (ChR2-eYFP) was virally expressed by stereotaxic injection into the BLA, vHipp or mPFC of BAC transgenic reporter mice (Fig. 2a). Retrograde labelling with cholera toxin subunit B in the dorso- or ventromedial NAc shell confirmed these regions as providing major afferents (Extended Data Fig. 2a), whereas anterograde labelling of different inputs with distinct fluorescent markers identified the juxtaposition of fibres in the NAc (Extended Data Fig. 3), in agreement with studies reporting the convergence of inputs onto the same MSN^{25–27}. Whole-cell recordings from mice infected with ChR2-eYFP in each region confirmed that inputs were excitatory (Extended Data Fig. 2c). Input and cell-type-specific plasticity were then evaluated *ex vivo* in the NAc shell from mice that self-administered cocaine or saline after 1 month of withdrawal.

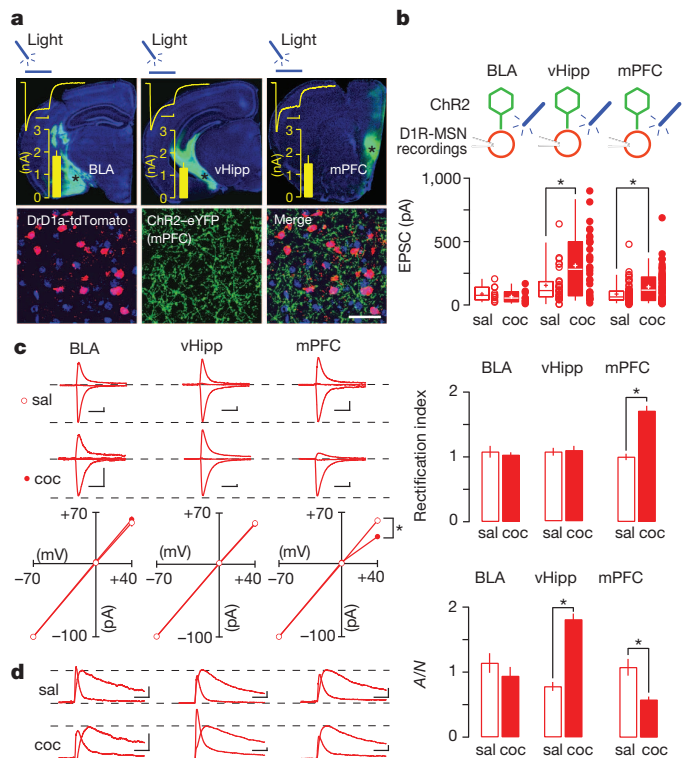


Figure 2 | Withdrawal from cocaine self-administration evokes input-specific plasticity in NAc D1R-MSNs. **a**, Top, images of BLA, vHipp and mPFC infected with ChR2-eYFP, with example traces and mean peak amplitudes of photocurrents (100 ms light pulses). Scale bars, 50 ms, 50 pA. Bottom, confocal image of NAc shell from a Drd1a-tdTomato mouse infected with ChR2 in the mPFC, as used for input and cell-type-specific recordings. Cell nuclei are stained with Hoechst. Scale bar, 100 μ m. **b**, Top, schematic of whole-cell recordings of D1R-MSNs from mice infected with ChR2 in the BLA (left), vHipp (centre) or mPFC (right). Bottom, cocaine (coc) self-administration increased the mean amplitude of 4 ms light-evoked EPSCs at vHipp and mPFC synapses ($t_{62} = 3.12$, $*P < 0.01$, $n = 30/34$ for saline (sal)/cocaine and $t_{120} = 3.0$, $*P < 0.01$, $n = 66/56$, respectively), but did not change BLA synapses ($t_{18} = 0.88$, $P = 0.39$; $n = 11/9$). **c**, For each input, example traces are shown (top), with *I/V* plots (bottom) and group mean rectification index data (right). Cocaine decreased normalized AMPAR-EPSCs at +40 mV from mPFC ($t_{19} = 4.16$, $*P < 0.01$, $n = 8/13$ for saline/cocaine) but not from BLA or vHipp inputs ($t_{11} = 0.67$, $P = 0.52$, $n = 5/8$ and $t_{20} = 0.18$, $P = 0.86$, $n = 9/13$, respectively). The rectification index was increased at mPFC synapses ($t_{19} = 6.9$, $*P \leq 0.001$), but not at BLA or vHipp synapses ($t_{11} = 0.58$, $P = 0.57$ and $t_{20} = 0.22$, $P = 0.83$, respectively). Scale bars, 20 ms, 20 pA. **d**, The *A/N* ratio was decreased by cocaine self-administration at mPFC synapses ($t_{19} = -3.59$, $P < 0.01$), but increased at vHipp synapses ($t_{20} = 8.33$, $P < 0.001$) and was unchanged at BLA synapses ($t_{11} = 0.94$, $P = 0.36$). $*P < 0.05$. Scale bars, 20 ms, 20 pA. Error bars, s.e.m.

Recordings of light-evoked AMPAR-EPSCs first confirmed that the strongest input onto the NAc arises from the hippocampus²⁴ and that cocaine self-administration evoked a significant potentiation of AMPAR-EPSC amplitudes only at vHipp and mPFC inputs onto D1R-MSNs (Fig. 2b). No change was observed at any input onto D2R-MSNs (Extended Data Fig. 4a). Remarkably, rectification of the current–voltage (I/V) curve was detected only at mPFC to D1R-MSN synapses in mice that self-administered cocaine, but not at vHipp or BLA to NAc synapses (Fig. 2c). Thus, cocaine self-administration triggered the insertion of CP-AMPA receptors only at mPFC to D1R-MSN synapses. Confirming findings with electrical stimulation, I/V curves were linear for all inputs onto D2R-MSNs in mice that self-administered cocaine (Extended Data Fig. 4b). For the A/N ratio, in mice that self-administered cocaine it was decreased at mPFC to D1R-MSN synapses (consistent with the poor conductance of CP-AMPA receptors at +40 mV), but increased at vHipp to D1R-MSN synapses and unaffected at BLA synapses (Fig. 2d). Cocaine self-administration evoked no change in the A/N ratio at any input onto D2R-MSNs (Extended Data Fig. 4c). Note that in baseline conditions (that is, mice that self-administered saline) both the rectification index and AMPAR/NMDA ratios were similar across all inputs onto D1R- and D2R-MSNs, as predicted from electrical recordings. Collectively, these results demonstrate that cocaine self-administration and withdrawal results in contrasting forms of plasticity at specific inputs onto the same accumbal D1R-MSN.

Homosynaptic effects of optogenetic protocols

Having identified specific inputs onto NAc shell D1R-MSNs that express drug-evoked plasticity, we wanted to test for a causal link to cue-associated

drug seeking. To this end, we aimed to develop optogenetic protocols *ex vivo* that could restore basal synaptic transmission (Fig. 3a, f). However, more than a complete erasure of cocaine-evoked plasticity, we sought to parse the relationship between plasticity at identified synapses to cue-associated seeking behaviour.

Because synapses were essentially potentiated after cocaine self-administration, optogenetic protocols were used that could trigger long-term depression (LTD). When recording light-evoked AMPAR-EPSCs selectively at vHipp to D1R-MSNs, application of a 1 Hz NMDAR-dependent LTD protocol²⁸ significantly depressed EPSCs both in saline and in cocaine self-administration groups (Fig. 3b). At the same input, a 13 Hz extrasynaptic metabotropic glutamate receptor (mGluR)-dependent LTD protocol (Extended Data Fig. 5a²⁹) triggered a depression in the cocaine self-administration group that was significantly attenuated compared with controls (Fig. 3c). The consequence of applying either protocol on cocaine-evoked plasticity at vHipp to NAc synapses (that is, homosynaptic effects) was then examined. As described above, CP-AMPA receptors were not present at vHipp to NAc synapses after cocaine self-administration and neither the 1 nor 13 Hz vHipp protocol further altered the linear I/V curve or rectification index at this input (Fig. 3d). Remarkably, however, the 1 Hz, but not the 13 Hz, vHipp protocol normalized the cocaine-evoked increase in the A/N ratio at this input (Fig. 3e). Note that in the group that self-administered saline, the 1 or 13 Hz vHipp protocols had little impact on the A/N ratio at these synapses, which was already low at baseline (Fig. 3e).

These experiments were repeated, but now isolating mPFC to D1R-MSN synapses (Fig. 3f). The 1 Hz mPFC protocol only slightly depressed AMPAR-EPSCs in the cocaine self-administration group, whereas the

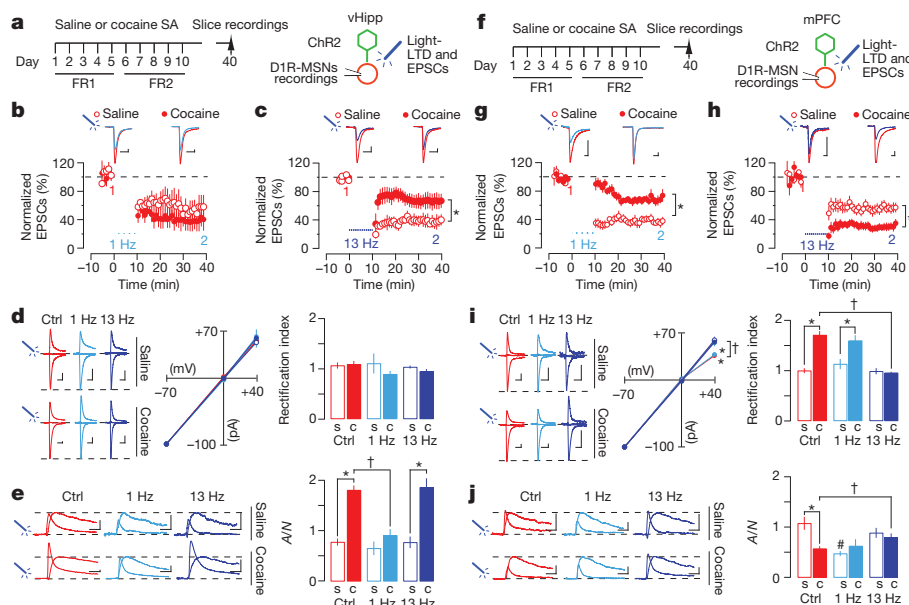


Figure 3 | Homosynaptic effects of optogenetic protocols applied *ex vivo* on D1R-MSN plasticity. **a**, Schematic of experiment for **b–e**; ChR2 in vHipp. **b**, Graph of normalized light-evoked EPSCs across time (bottom: each point represents mean of six sweeps), with example traces (top: mean of 20 sweeps) before (1) and after (2) the LTD protocol (4 ms pulses at 1 Hz, 10 min). One month after cocaine self-administration, the efficiency of the 1 Hz LTD protocol was not modified ($56.3 \pm 14.7\%$ to $38.6 \pm 12.2\%$, $t_7 = 0.89$, $P = 0.4$; $n = 5/4$). **c**, As for **b**, but with a 13 Hz protocol (4 ms pulses at 13 Hz, 10 min). The efficiency of this protocol was reduced in mice that self-administered cocaine ($39.2 \pm 6.7\%$ to $69.5 \pm 10.1\%$, $t_9 = 2.57$, $*P = 0.03$; $n = 6/5$). **d**, Example traces (left) of light-evoked AMPAR-EPSCs recorded at -70 , 0 and $+40$ mV, with I/V plot (middle) and group mean rectification index data (right) before (Ctrl) and after the 1 or 13 Hz light protocol, both in saline (s) and cocaine (c) self-administered groups. AMPAR composition was not modified by cocaine or light protocols (saline/cocaine for Ctrl ($n = 9/13$), 1 Hz (6/4), 13 Hz (8/5)). **e**, For the same cells in **d**, example traces (left), with mean A/N

ratios (right) before or after the 1 or 13 Hz protocol. Planned comparisons, after analysis of variance (ANOVA), by t -test, †, $*P \leq 0.05$. **f**, Schematic of experiment for **g–j**; ChR2 in the mPFC. **g**, The 1 Hz protocol efficiency was reduced in mice that self-administered cocaine ($43 \pm 5.5\%$ to $74 \pm 3.7\%$, $t_{17} = 4.9$, $*P < 0.001$; $n = 8/11$). **h**, The 13 Hz protocol efficiency was increased in mice that self-administered cocaine ($54 \pm 6.1\%$ to $29 \pm 4.7\%$, $t_{22} = 3.25$, $*P < 0.01$; $n = 13/11$). **i**, The 13 Hz but not 1 Hz protocol normalized cocaine-evoked changes in AMPAR-EPSCs at +40 mV and rectification index. Planned comparisons, after ANOVA, by t -test, †, $*P \leq 0.05$; (saline/cocaine for Ctrl ($n = 9/13$), 1 Hz (10/7), 13 Hz (10/6)). **j**, For the same cells as **i**, the cocaine-evoked decrease in A/N ratio was normalized by the 13 Hz, but not the 1 Hz, protocol. The 1 Hz protocol decreased A/N ratio in saline mice ($\#P < 0.05$). Planned comparisons, after ANOVA, by t -test, †, $*P \leq 0.05$. Note that control data are the same as shown in Fig. 2. Scale bars, 20 pA, 20 ms. Error bars, s.e.m.

depression was significantly larger in controls (Fig. 3g). This finding concurs with a previous study where NMDAR-dependent LTD was altered in ‘cocaine-addicted’ rats³⁰. The 13 Hz mPFC protocol was actually more efficient in the cocaine self-administration group (Fig. 3h), which is of particular interest because mGluR activation can remove CP-AMPA receptors at many synapses throughout the brain^{31–33}. Both protocols triggered comparable LTD of AMPAR-EPSCs in D2R-MSNs from saline and mice that self-administered cocaine (Extended Data Fig. 5b). The homosynaptic effects of these protocols on cocaine-evoked plasticity at mPFC to NAc synapses was then examined which, as described above, indicated the presence of CP-AMPA receptors. Consistent with LTD experiments, the 13 Hz, but not the 1 Hz, mPFC protocol normalized both the rectifying *I/V* curve and the depressed *A/N* ratio (Fig. 3i, j), pointing to removal of CP-AMPA receptors from mPFC to D1R-MSN synapses. In the group that self-administered saline, the 1 Hz, but not the 13 Hz, mPFC protocol significantly reduced the *A/N* ratio, whereas the rectification index remained unchanged in either case.

Heterosynaptic effects of optogenetic protocols

After evaluating the 1 and 13 Hz protocols on light-evoked homosynaptic transmission, the possibility of heterosynaptic effects was explored *ex vivo* (that is, normalization of cocaine-evoked plasticity at an input other than which the protocol was applied). Indeed, *in vivo* recordings have demonstrated that activation of one excitatory NAc input can trigger heterosynaptic plasticity²⁷.

Optogenetic LTD protocols were applied onto slices at vHipp or mPFC to NAc inputs but EPSCs were evoked with electrical stimulation, thus recruiting transmission from multiple afferents (Fig. 4a). The cocaine-evoked rectification of AMPAR transmission was restored by the 13 Hz protocol, whether applied at vHipp or mPFC to NAc synapses (Fig. 4b). Because rectification was only found at mPFC to D1R-MSN synapses, the 13 Hz vHipp protocol must have triggered normalization of this synapse heterosynaptically, most probably by activating mGluRs

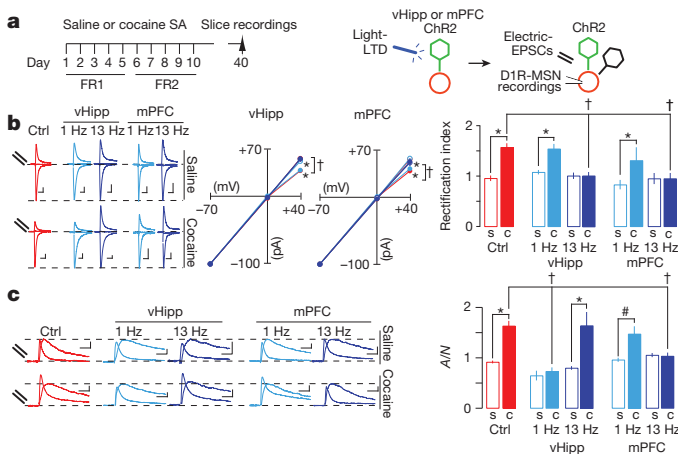


Figure 4 | Heterosynaptic effects of optogenetic protocols applied *ex vivo* on D1R-MSN plasticity. **a**, Schematic of experiment. **b**, Example traces (left) of electrically evoked AMPAR-EPSCs recorded at -70 , 0 and $+40$ mV, with *I/V* plots (middle) and grouped mean rectification index data (right) before (Ctrl) or after light protocols (1 or 13 Hz) were applied with ChR2 in the vHipp or mPFC. The 13 Hz but not 1 Hz light protocol applied at vHipp or mPFC synapses normalized AMPA-EPSCs at $+40$ mV and rectification index (planned comparisons, after ANOVAs, with *t*-tests: $^* \dagger P \leq 0.05$; (saline/cocaine for Ctrl ($n = 9/41$), for vHipp 1 Hz (6/8) and 13 Hz (8/8), for mPFC 1 Hz (12/9) and 13 Hz (15/8))). **c**, For the same cells shown in **b**, example traces (left) and group mean *A/N* ratios (right) before or after the 1 or 13 Hz protocols. The 1 Hz vHipp or the 13 Hz mPFC protocol normalized the cocaine-evoked increase in *A/N* ratio, whereas the *A/N* ratio remained elevated after the 13 Hz vHipp protocol or the 1 Hz mPFC protocol (planned comparisons, after ANOVAs, with *t*-tests: $\dagger, ^* P < 0.05$ and $\# P = 0.07$). Note that control data are the same as shown in Fig. 1. Scale bars, 20 pA, 20 ms. Error bars, s.e.m.

at neighbouring synapses through glutamate spillover or intracellular signalling. For the *A/N* ratio, which was increased in the cocaine self-administration group when recorded with electrical stimulation, normalization was observed using the 1 Hz vHipp protocol (Fig. 4c). This probably reflected a homosynaptic effect as reported above (see Fig. 3e). However, the 13 Hz mPFC protocol, in addition to removing rectifying AMPARs, also restored the *A/N* ratio; a heterosynaptic effect probably occurring through glutamate spillover activating NMDARs at vHipp to D1R-MSN synapses. Note that the 13 Hz vHipp protocol, in contrast to its heterosynaptic effect on the rectification index, did not elicit a homosynaptic reduction in the *A/N* ratio, possibly because NMDAR activation was too strong to elicit depression^{34,35}. Because our initial validations were performed *ex vivo*, we also confirmed that optogenetic protocols were efficient in normalizing cocaine-evoked plasticity when applied *in vivo* (Extended Data Figs 6 and 7, which include extra discussion). Taken together, this approach led to an advantageous situation to test the causality of contrasting forms of drug-evoked plasticity in cue-associated cocaine seeking, because plasticity at mPFC or vHipp to D1R-MSNs could be restored separately using the 13 Hz vHipp or the 1 Hz vHipp protocol, respectively, or together by using the 13 Hz mPFC protocol.

Causal link to components of cocaine seeking

Now we applied optogenetic protocols in self-administration mice to test directly the causality between drug-evoked plasticity at identified inputs and a drug-adaptive behaviour relevant to addiction. After 1 month of withdrawal from self-administration, mice underwent a cue-associated seeking test, a rodent model of relapse, with optogenetic protocols applied once, 4 h before the test (Fig. 5a, b).

The 1 Hz vHipp protocol (that is, reversing cocaine-evoked plasticity only at vHipp to D1R-MSNs) significantly reduced cue-associated lever pressing, a measure of response vigour, although cocaine seeking per se was still present. The 13 Hz vHipp protocol (that is, inducing a heterosynaptic reversal of plasticity at mPFC to D1R-MSNs) led to increased inactive lever responding, pointing to impaired action–outcome response

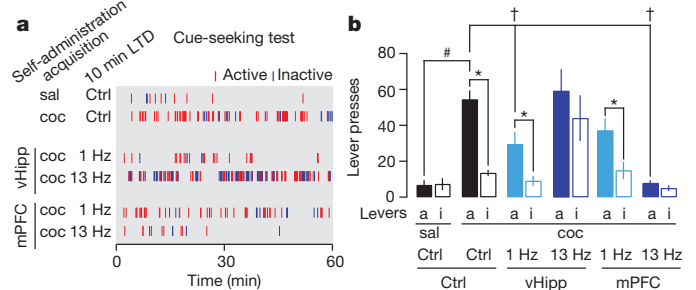


Figure 5 | Linking cocaine-evoked plasticity at identified inputs to specific components of cue-associated cocaine seeking. **a**, Raster plots showing active and inactive lever presses during a cue-associated seeking session. **b**, Group mean data showing active (a) and inactive (i) lever presses. Seeking was robust in control mice that self-administered cocaine (active versus inactive lever, $t_{43} = 9.5$, $^* P < 0.001$; $n = 11/44$, saline/cocaine; active lever to saline control group, after ANOVA, by *t*-test: $t_{53} = 4.6$, $\# P < 0.001$). Seeking was present after the 1 Hz vHipp protocol ($t_{10} = 3.6$, $^* P < 0.01$), but active lever responses were significantly diminished (versus cocaine control group, after ANOVA, by *t*-test: $t_{53} = 2.3$, $\dagger P < 0.05$; $n = 11/44$). Lever discrimination was lost after the 13 Hz vHipp protocol ($t_8 = 1.99$, $P > 0.05$), and inactive lever responses were significantly increased (versus cocaine control group, after ANOVA, by *t*-test: $t_{51} = 4.48$, $P < 0.001$; $n = 9/44$). Seeking was present after the 1 Hz mPFC protocol and did not differ from the cocaine controls (versus cocaine control groups by ANOVA: lever, protocol and lever \times protocol interaction all non-significant; $n = 11/44$). Active lever responding was reduced after the 13 Hz mPFC protocol (versus cocaine control group, after ANOVA, by *t*-test: $t_{52} = 4.3$, $^* P < 0.001$; $n = 10/44$) and lever discrimination was lost (active versus inactive levers by *t*-test, $t_9 = 1.7$, $P > 0.1$, $n = 10$). See Extended Data Table 1 for complete statistics. Error bars, s.e.m.

discrimination. The 1 Hz mPFC protocol (that is, no effect on cocaine-evoked plasticity) was without effect on seeking behaviour. Finally, the 13 Hz mPFC protocol (that is, normalizing both inputs) abolished seeking behaviour (Fig. 5a, b). To examine the persistence of this effect, the same mice were tested for cue-associated cocaine seeking 1 week later without further optogenetic intervention. Seeking behaviour remained absent in mice that received the 13 Hz mPFC protocol (Extended Data Figs 8a, b and 9). Taken together, these data demonstrate that cocaine-evoked plasticity at two inputs onto NAc D1R-MSNs is required for the complete expression of cue-associated seeking, whereas each form of contrasting plasticity is causally related to a different component of the seeking behaviour, namely the vigour of the seeking response and the ability to discriminate cocaine- from non-cocaine-directed actions.

We performed extra tests to control for the behavioural specificity of optogenetic interventions. First, optogenetic removal of cocaine-evoked plasticity did not preclude the acquisition of further reward-related instrumental learning (Extended Data Fig. 8c, which includes further description). Second, the 13 Hz mPFC protocol did not affect cue-associated food seeking behaviour in a cohort of mice that were previously trained to self-administer sucrose pellets (Extended Data Fig. 8d–f, which includes further description), suggesting that this protocol is selective for cocaine-evoked plasticity necessary for cocaine seeking against plasticity that may correlate with food seeking^{36,37}.

Discussion

A striking feature of this study is the input-specific expression mechanism of drug-evoked plasticity. In the same D1R-MSNs, synapses that belong to the mPFC input show rectifying AMPAR-EPSCs reflecting the insertion of GluA2-lacking CP-AMPA receptors, whereas at neighbouring vHipp synapses an increased *A/N* ratio and significantly larger EPSC amplitude indicates the insertion of more GluA2-containing AMPARs. Moreover, such forms of plasticity were absent at other synapses and in D2R-MSNs, although these neurons may still contribute to features of addiction³⁸. Why are some synapses susceptible to cocaine-evoked plasticity and why do the expression mechanisms differ between inputs? These findings may reflect a complex induction process, requiring specific neuronal activity patterns coinciding with high levels of mesolimbic dopamine during drug exposure. Indeed, different drug self-administration histories may favour the induction of synaptic plasticity at other NAc inputs, such as the BLA³⁹. Another possibility is that contrasting expression mechanisms reflect differences in the quality of basal synaptic transmission between cortical and limbic inputs onto NAc MSNs²⁴, or differences in the sensitivity of synapses to be influenced by the coincidence of converging glutamate and dopamine signals involving D1R signalling^{11,27}.

Here we focus on the vHipp and mPFC input onto D1R-MSNs, taking advantage of endogenous depression mechanisms (for example, NMDAR or mGluR activation^{28,29,40}) to restore normal transmission in each input separately or both inputs together. Although the 1 Hz LTD protocol is sufficient to recruit NMDARs on the activated input, trains of action potentials (for example, 13 Hz stimulation) are required to release sufficient amounts of glutamate to activate perisynaptically located mGluRs, even at neighbouring inputs. mGluR-LTD in the NAc is expressed both pre- and postsynaptically^{29,33,41}, but what most likely matters is that mGluR-LTD is an efficient mechanism to remove GluA2-lacking AMPARs, just as in other central nervous system synapses^{31,32,42}. It is therefore not surprising that the 1 Hz mPFC protocol failed to normalize rectification index and had no behavioural effect. The 1 Hz vHipp protocol normalized the *A/N* ratio at vHipp to D1R-MSN synapses and significantly reduced the vigour with which the animal pressed the active lever in search of cocaine. Thus, cocaine-evoked plasticity at vHipp afferents to NAc D1R-MSNs may enhance recognition of the correct context in which cocaine can be obtained. In the absence of this plasticity, context recognition may be impaired and the certainty of actions reduced. Meanwhile, removal of CP-AMPA receptors from mPFC to D1R-MSN synapses led to a failure of discrimination between the cocaine-associated lever and a second lever on which responding had no consequence. This

establishes cocaine-evoked plasticity at mPFC afferents to NAc D1R-MSNs as necessary to allow correct action–outcome selection during seeking. Finally, restoring transmission in both inputs abolished cue-induced cocaine seeking. Thus, cocaine-evoked plasticity at multiple inputs, with distinct expression mechanisms that change both the efficacy and quality of transmission, are collectively necessary for the full expression of cue-associated drug-seeking behaviour.

Previous studies have recognized the importance of NAc excitatory transmission in drug-adaptive behaviours using systemic or local applications of pharmacological agents that are active during the behavioural test^{20,21,43}. However, a key difference in the present study is that optogenetic protocols were applied outside the test and remained effective 1 week later. Thus, findings here provide support for a model whereby a cocaine memory trace commandeers accumbal integration to control core components of relapse. Co-opting endogenous plasticity mechanisms emerges as a radically new way to modify behaviour and may serve as a blueprint for defining synaptic causalities in other synaptic disorders.

METHODS SUMMARY

Mice learned to self-administer cocaine or saline during once-daily 2 h sessions for 10 consecutive days²². In each self-administration session, mice could respond on either an active lever that resulted in a single infusion (0.75 mg kg⁻¹ cocaine or saline) paired with a 5 s cue light and followed by a 20 s time-out period, or a second inactive lever that had no consequence. Responding was maintained under a fixed-ratio one schedule (one active lever press gives one infusion) during sessions 1–5, and fixed-ratio two schedule during sessions 6–10. After the final self-administration session, mice were retained in their home cage for 1 month of forced withdrawal. The 60 min test of cue-associated cocaine seeking took place in the same box where self-administration training occurred. Responses on the active lever now triggered a 5 s illumination of the cocaine-associated cue light, but without intravenous infusion, whereas inactive lever responses had no consequence. Optogenetic protocols were applied once *in vivo*, in the home cage, through bilaterally implanted optical fibres targeting the NAc shell 4 h before the seeking test, or before animals were killed for *ex vivo* recordings. For whole-cell patch clamp recordings, the rectification index was calculated after measuring light-evoked EPSC amplitudes at different holding potentials (–70, 0 and +40 mV) in the presence of (D)-2-amino-5-phospho-novaleric acid (AP5; 50 μM). The *A/N* ratio was calculated at +40 mV with the AMPAR component pharmacologically isolated using AP5 (50 μM) and the NMDAR-EPSC component determined by subtraction. When using Chr2–eYFP in BAC transgenic mice, D2R-MSNs were identified as D2R–eGFP (enhanced green fluorescent protein)-positive neurons in *Drd2*–eGFP mice or as tomato-negative neurons in *Drd1a*–tdTomato mice, whereas D1R-MSNs were always identified as tomato-positive cells. This approach was validated in a previous report²⁸.

Online Content Any additional Methods, Extended Data display items and Source Data are available in the online version of the paper; references unique to these sections appear only in the online paper.

Received 24 January; accepted 17 March 2014.

1. Robbins, T. W. & Everitt, B. J. Neurobehavioural mechanisms of reward and motivation. *Curr. Opin. Neurobiol.* **6**, 228–236 (1996).
2. Berridge, K. C. & Kringelbach, M. L. Neuroscience of affect: brain mechanisms of pleasure and displeasure. *Curr. Opin. Neurobiol.* **23**, 294–303 (2013).
3. Humphries, M. D. & Prescott, T. J. The ventral basal ganglia, a selection mechanism at the crossroads of space, strategy, and reward. *Prog. Neurobiol.* **90**, 385–417 (2010).
4. Papp, E. *et al.* Glutamatergic input from specific sources influences the nucleus accumbens-ventral pallidum information flow. *Brain Struct. Funct.* **217**, 37–48 (2012).
5. Everitt, B. J. & Robbins, T. W. Neural systems of reinforcement for drug addiction: from actions to habits to compulsion. *Nature Neurosci.* **8**, 1481–1489 (2005).
6. Kalivas, P. W. & Volkow, N. D. The neural basis of addiction: a pathology of motivation and choice. *Am. J. Psychiatry* **162**, 1403–1413 (2005).
7. Gangarossa, G. *et al.* Distribution and compartmental organization of GABAergic medium-sized spiny neurons in the mouse nucleus accumbens. *Front. Neural Circuits* **7**, 22 (2013).
8. MacAskill, A. F., Little, J. P., Cassel, J. M. & Carter, A. G. Subcellular connectivity underlies pathway-specific signaling in the nucleus accumbens. *Nature Neurosci.* **15**, 1624–1626 (2012).
9. Smith, R. J., Lobo, M. K., Spencer, S. & Kalivas, P. W. Cocaine-induced adaptations in D1 and D2 accumbens projection neurons (a dichotomy not necessarily synonymous with direct and indirect pathways). *Curr. Opin. Neurobiol.* **23**, 546–552 (2013).

10. Freund, T. F., Powell, J. F. & Smith, A. D. Tyrosine hydroxylase-immunoreactive boutons in synaptic contact with identified striatonigral neurons, with particular reference to dendritic spines. *Neuroscience* **13**, 1189–1215 (1984).
11. Goto, Y. & Grace, A. A. Limbic and cortical information processing in the nucleus accumbens. *Trends Neurosci.* **31**, 552–558 (2008).
12. Cerovic, M., d'Isa, R., Tonini, R. & Brambilla, R. Molecular and cellular mechanisms of dopamine-mediated behavioral plasticity in the striatum. *Neurobiol. Learn. Mem.* **105**, 63–80 (2013).
13. Sadoris, M. P., Sugam, J. A., Cacciapaglia, F. & Carelli, R. M. Rapid dopamine dynamics in the accumbens core and shell: learning and action. *Front. Biosci. (Elite Ed.)* **5**, 273–288 (2013).
14. Schultz, W. Potential vulnerabilities of neuronal reward, risk, and decision mechanisms to addictive drugs. *Neuron* **69**, 603–617 (2011).
15. Di Chiara, G. & Bassareo, V. Reward system and addiction: what dopamine does and doesn't do. *Curr. Opin. Pharmacol.* **7**, 69–76 (2007).
16. Hyman, S. Addiction: a disease of learning and memory. *Am. J. Psychol.* **162**, 1414–1422 (2005).
17. Lüscher, C. & Malenka, R. C. Drug-evoked synaptic plasticity in addiction: from molecular changes to circuit remodeling. *Neuron* **69**, 650–663 (2011).
18. Kourrich, S., Rothwell, P. E., Klug, J. R. & Thomas, M. J. Cocaine experience controls bidirectional synaptic plasticity in the nucleus accumbens. *J. Neurosci.* **27**, 7921–7928 (2007).
19. Ortinski, P. I., Vassoler, F. M., Carlson, G. C. & Pierce, R. C. Temporally dependent changes in cocaine-induced synaptic plasticity in the nucleus accumbens shell are reversed by D1-like dopamine receptor stimulation. *Neuropsychopharmacology* **37**, 1671–1682 (2012).
20. Cornish, J. L. & Kalivas, P. W. Glutamate transmission in the nucleus accumbens mediates relapse in cocaine addiction. *J. Neurosci.* **20**, RC89 (2000).
21. Conrad, K. L. et al. Formation of accumbens GluR2-lacking AMPA receptors mediates incubation of cocaine craving. *Nature* **454**, 118–121 (2008).
22. Ambroggi, F. et al. Stress and addiction: glucocorticoid receptor in dopamine-receptive neurons facilitates cocaine seeking. *Nature Neurosci.* **12**, 247–249 (2009).
23. Liu, S. J. & Zukin, R. S. Ca²⁺-permeable AMPA receptors in synaptic plasticity and neuronal death. *Trends Neurosci.* **30**, 126–134 (2007).
24. Britt, J. P. et al. Synaptic and behavioral profile of multiple glutamatergic inputs to the nucleus accumbens. *Neuron* **76**, 790–803 (2012).
25. French, S. J. & Totterdell, S. Hippocampal and prefrontal cortical inputs monosynaptically converge with individual projection neurons of the nucleus accumbens. *J. Comp. Neurol.* **446**, 151–165 (2002).
26. French, S. J. & Totterdell, S. Individual nucleus accumbens-projection neurons receive both basolateral amygdala and ventral subicular afferents in rats. *Neuroscience* **119**, 19–31 (2003).
27. Goto, Y. & Grace, A. A. Dopamine-dependent interactions between limbic and prefrontal cortical plasticity in the nucleus accumbens: disruption by cocaine sensitization. *Neuron* **47**, 255–266 (2005).
28. Pascoli, V., Turiault, M. & Lüscher, C. Reversal of cocaine-evoked synaptic potentiation resets drug-induced adaptive behaviour. *Nature* **481**, 71–75 (2011).
29. Robbe, D., Kopf, M., Remaury, A., Bockaert, J. & Manzoni, O. J. Endogenous cannabinoids mediate long-term synaptic depression in the nucleus accumbens. *Proc. Natl Acad. Sci. USA* **99**, 8384–8388 (2002).
30. Kasanetz, F. et al. Transition to addiction is associated with a persistent impairment in synaptic plasticity. *Science* **328**, 1709–1712 (2010).
31. Lüscher, C. & Huber, K. M. Group 1 mGluR-dependent synaptic long-term depression: mechanisms and implications for circuitry and disease. *Neuron* **65**, 445–459 (2010).
32. Clem, R. L. & Huganir, R. L. Calcium-permeable AMPA receptor dynamics mediate fear memory erasure. *Science* **330**, 1108–1112 (2010).
33. McCutcheon, J. E. et al. Group 1 mGluR activation reverses cocaine-induced accumulation of calcium-permeable AMPA receptors in nucleus accumbens synapses via a protein kinase C-dependent mechanism. *J. Neurosci.* **31**, 14536–14541 (2011).
34. Bienenstock, E. L., Cooper, L. N. & Munro, P. W. Theory for the development of neuron selectivity: orientation specificity and binocular interaction in visual cortex. *J. Neurosci.* **2**, 32–48 (1982).
35. Lüscher, C. & Malenka, R. C. NMDA receptor-dependent long-term potentiation and long-term depression (LTP/LTD). *Cold Spring Harb. Perspect. Biol.* **4**, a005710 (2012).
36. Counotte, D. S., Schiefer, C., Shaham, Y. & O'Donnell, P. Time-dependent decreases in nucleus accumbens AMPA/NMDA ratio and incubation of sucrose craving in adolescent and adult rats. *Psychopharmacology* **231**, 1675–1684 (2013).
37. Smith, D. G. & Robbins, T. W. The neurobiological underpinnings of obesity and binge eating: a rationale for adopting the food addiction model. *Biol. Psych.* **9**, 804–810 (2013).
38. Bock, R. et al. Strengthening the accumbal indirect pathway promotes resilience to compulsive cocaine use. *Nature Neurosci.* **16**, 632–638 (2013).
39. Lee, B. R. et al. Maturation of silent synapses in amygdala-accumbens projection contributes to incubation of cocaine craving. *Nature Neurosci.* **16**, 1644–1651 (2013).
40. Kombian, S. B. & Malenka, R. C. Simultaneous LTP of non-NMDA- and LTD of NMDA-receptor-mediated responses in the nucleus accumbens. *Nature* **368**, 242–246 (1994).
41. Grueter, B. A., Brasnjo, G. & Malenka, R. C. Postsynaptic TRPV1 triggers cell type-specific long-term depression in the nucleus accumbens. *Nature Neurosci.* **13**, 1519–1525 (2010).
42. Bellone, C. & Lüscher, C. Cocaine triggered AMPA receptor redistribution is reversed *in vivo* by mGluR-dependent long-term depression. *Nature Neurosci.* **9**, 636–641 (2006).
43. Koya, E. et al. Role of ventral medial prefrontal cortex in incubation of cocaine craving. *Neuropharmacology* **56** (suppl. 1), 177–185 (2009).

Acknowledgements We thank D. Huber and M. Brown as well the members of the Lüscher laboratory for discussion and comments on the manuscript, and A. Hiver for assisting in animal surgery. This work was financed by a grant from the Swiss National Science Foundation, the National Center of Competence in Research (NCCR) 'SYNAPSY - The Synaptic Bases of Mental Diseases' of the Swiss National Science Foundation and a European Research Council advanced grant (MeSSI). J.T. is supported by an MD-PhD grant of the Swiss Confederation. The E.V. laboratory was supported by an Avenir grant (Inserm) and by the Agence Nationale de la Recherche.

Author Contributions V.P. performed all the *in vitro* electrophysiological recordings. J.T. performed all surgery and behavioural experiments with the assistance of E.C.O.C. J.E. and E.V. performed the fluorescence immunohistochemical experiments. C.L., P.V., J.T. and E.C.O.C. designed the study, and C.L. wrote the manuscript with the help of all authors.

Author Information Reprints and permissions information is available at www.nature.com/reprints. The authors declare no competing financial interests. Readers are welcome to comment on the online version of the paper. Correspondence and requests for materials should be addressed to C.L. (christian.luscher@unige.ch).

METHODS

Animals. Mice were C57BL/6 or heterozygous BAC transgenic mice in which tomato expression was driven by D1R (Drd1a-tdTomato from Jackson Laboratories) gene regulatory elements or eGFP driven by D2R (Drd2-eGFP from GENSAT) gene regulatory elements. Males and females were used. Transgenic mice had been backcrossed in the C57BL/6 line for a minimum of four generations. Mice were single housed after surgery. All animals were kept in a temperature- and humidity-controlled environment with a 12 h light/12 h dark cycle (lights on at 7:00). All procedures were approved by the Institutional Animal Care and Use Committee of the University of Geneva.

Stereotaxic injections. AAV1-CAG-ChR2-eYFP (eYFP; also called venus) or AAV1-CAG-eYFP (for control mice) produced at the University of North Carolina (Vector Core Facility) was injected into the mPFC (focusing on the infralimbic area), vHipp or BLA of 5- to 6-week-old mice. Anaesthesia was induced at 5% and maintained at 2.5% isoflurane (w/v) (Baxter AG) during the surgery. The animal was placed in a stereotaxic frame (Angle One) and craniotomies were performed using stereotaxic coordinates adapted from a mouse brain atlas⁴⁴ (for mPFC: anterior–posterior = +1.9; medial–lateral = ± 0.3; dorsal–ventral (from the surface of the brain) = -2.5; for vHipp: anterior–posterior = -3.5; medial–lateral = ± 2.8; dorsal–ventral = -4.2; for BLA: anterior–posterior = -1.4; medial–lateral = ± 3.0; dorsal–ventral = -3.8). Injections of virus (0.5 µl per injection site) used graduated pipettes (Drummond Scientific Company), broken back to a tip diameter of 10–15 µm, at an infusion rate of ~0.05 µl min⁻¹. Injections of ChR2 were made a minimum of 1 week before the self-administration surgery, and thus optogenetic manipulations typically occurred no sooner than 7 weeks after the injection. For anterograde tracing studies, 6- to 8-week-old C57BL/6J mice were infected with both AAV5-EF1α-mCherry in the mPFC and AAV5-EF1α-eYFP in the vHipp to allow observation of multiple inputs into NAc.

For retrograde tract-tracing studies, mice were stereotaxically injected with the retrograde tracer, cholera toxin subunit B conjugated to a fluorescent marker (cholera toxin subunit B, Alexa Fluor 594 conjugate, Molecular Probes). Microinjection needles were placed into the NAc medio-dorsal (anterior–posterior = +1.18; medial–lateral = +0.5; dorsal–ventral = -3.7) or NAc medio-ventral (anterior–posterior = +1.18; medial–lateral = +0.5; dorsal–ventral = -4.2) and 0.5 µl was injected over 5 min. The injector was left in place for an extra 5 min to allow for diffusion of cholera toxin subunit B particles away from the injection site. Animals returned to their home cages for 14 days before tissue preparation.

Tissue preparation and immunofluorescence. Mice were rapidly anaesthetized with pentobarbital (500 mg kg⁻¹, intraperitoneally, Sanofi-Aventis) and transcardially perfused with 4% (w/v) paraformaldehyde in 0.1 M sodium phosphate buffer (pH 7.5) (ref. 45). Brains were post-fixed overnight in the same solution and stored at 4 °C. Thirty-micrometre-thick sections were cut with a vibratome (Leica) and stored at -20 °C in a solution containing 30% (v/v) ethylene glycol, 30% (v/v) glycerol, and 0.1 M sodium phosphate buffer, until they were processed for immunofluorescence. Sections were processed as follows. Free-floating sections were rinsed in Tris-buffered saline (TBS: 0.25 M Tris and 0.5 M NaCl, pH 7.5), incubated for 5 min in TBS containing 3% H₂O₂ and 10% methanol (v/v), and then rinsed three times 10 min in TBS. After incubation for 15 min in 0.2% (v/v) Triton X-100 in TBS, sections were rinsed three times in TBS again. Sections were then incubated for 1 h in a solution of BSA 3% in TBS. Finally, they were incubated 72 h at 4 °C with the primary antibodies mouse anti-DARPP-32 (1:1,000, a gift from P. Greengard, mouse monoclonal clone C54 (ref. 46)) and rabbit anti-RFP (1:1,000, Medical & Biological Laboratories, rabbit polyclonal, lot 042). After incubation with the primary antibodies, sections were rinsed three times for 10 min in TBS and incubated for 45 min with goat Cy3- and Cy5-coupled secondary antibodies (1:400, Jackson ImmunoResearch, lot 114787 and Life Technologies 1305923). Sections were rinsed for 10 min twice in TBS and twice in tris-buffer (0.25 M Tris) before mounting in 1,4-diazabicyclo-[2.2.2]-octane (DABCO, Sigma-Aldrich). Double- or triple-labelled images from each region of interest were obtained using sequential laser scanning confocal microscopy (Zeiss LSM510 META). Photomicrographs were obtained with the following band-pass and long-pass filter settings: GFP (band-pass filter: 505–530), Cy3 (band-pass filter: 560–615) and Cy5 (long-pass filter 650). The objectives and the pinhole setting (1 airy unit) remained unchanged during the acquisition of a series for all images. The thickness of the optical section was ~1.6 µm with a ×20 objective and ~6 µm with a ×10 objective. GFP-labelled neurons were pseudo-coloured green and other immunoreactive neurons were pseudo-coloured red or blue. For images showing infected structure with AAV1-CAG-ChR2-eYFP, 30 µm-thick coronal sections were cut with a vibratome (Leica), stained with Hoechst (Sigma-Aldrich) and mounted with Mowiol (Sigma-Aldrich). Full images of brain slices from mPFC, BLA and vHipp were obtained with a MIRAX (Carl Zeiss) system equipped with a Plan-Apochromat ×20/0.8 objective, together with 4',6-diamidino-2-phenylindole (DAPI) (emission: 455/50) and fluorescein isothiocyanate (FITC) (emission: 515–565) filters.

Implantation of jugular vein catheter. The surgical procedure was adapted from refs 47, 48. Mice were anaesthetized with a mix of ketamine (60 mg kg⁻¹, Ketalar) and xylazine (12 mg kg⁻¹, Rompun) solution. Catheters (CamCaths, model MIVSA) made of silicone elastomer tubing (outside diameter 0.63 mm, inside diameter 0.30 mm) were inserted 1.0–1.2 cm in the right jugular vein, about 5 mm from the pectoral muscle, to reach the right atrium. The other extremity of the catheter was placed subcutaneously in the mid-scapular region and connected to stainless steel tubing appearing outside the skin. Blood reflux in the tubing was checked to confirm correct placement of the catheter. Mice were allowed to recover for 3–5 days before the start of drug self-administration training and received antibiotics (Baytril 10%, 1 ml in 250 ml of water) in the drinking water during this period. Catheters were flushed daily with a heparin solution (Heparin 'Bichsel' in saline (30 IU) during the recovery period and just before and after each self-administration session.

Self-administration apparatus. All behavioural experiments were performed during the light phase and took place in mouse operant chambers (ENV-307A-CT, Med Associates) situated in sound-attenuating cubicle (Med Associates). Two retractable levers were present on both sides of one wall of the chamber and a food pellet dispenser was also present only for procedures involving food delivery. A cue-light was located above each lever and a house light was present in each chamber. During intravenous drug self-administration sessions, the stainless steel tubing of the catheter device was connected through a CoEx PE/PVC tubing (BCOEX-T25, Instech Solomon) to a swivel (Instech Solomon) and then an infusion pump (PHM-100, Med-Associates). The apparatus was controlled and data captured using a PC running MED-PC IV (Med-Associated).

Drug self-administration acquisition. Mice were deprived of food for 12 h before the first self-administration session to promote exploratory activity. No food shaping was undertaken and mice were given food access *ad libitum* after the first session. Each session was 120 min in duration and started with the illumination of the house light and the insertion of the two levers into the operant chamber. During the first five sessions, a single press on the active lever (termed fixed-ratio one, or FR1) resulted in an infusion of 0.75 mg kg⁻¹ of cocaine (cocaine hydrochloride, provided by the pharmacy of Geneva University Hospital, dissolved in 0.9% saline at 0.75 mg ml⁻¹ and delivered at 0.0177 ml s⁻¹ as a unit dose depending on the weight of the mouse) paired with a 5 s continuous illumination of the cue light above the active lever. Completion of the fixed-ratio also initiated a timeout period of 20 s during which cocaine was no longer available. For the next five sessions, two lever presses were needed to activate the infusion pump (FR2). The active lever (left or right lever) was randomly assigned for each mouse. To avoid an overdose of cocaine, a maximum of 45 infusions were allowed per session. Only mice having reached a stable rate of at least 70% of correct lever responses (number of active lever responses divided by total lever responses over the three last sessions of acquisition) were included in the study. Saline control mice undertook the same procedure as cocaine mice except that saline (NaCl 0.9% B. Braun) replaced cocaine infusions. After acquisition, mice were randomly attributed to either behaviour or electrophysiology experiments (except wild-type mice, which were only used in behaviour experiments). Recordings were never performed after cue-associated seeking tests to avoid confounding effects on synaptic transmission⁴⁹.

Optic fibre cannulation and *in vivo* optogenetic stimulation protocols. After completing the acquisition of self-administration, all mice were put in forced abstinence for 30 days in their home cage. At days 15–20, mice destined for seeking tests or *ex vivo* validation were bilaterally implanted with a chronically indwelling optic-fibre cannula (made in house as described in ref. 50) into the NAc (anterior–posterior = +1.5; medial–lateral = ± 1.6; dorsal–ventral = -3.9 with a 10° angle) using stereotaxic apparatus as described above. Two screws were fixed into the skull to support the implant, which was further secured with dental cement.

DPSS blue light lasers (MBL-473/50 mW; CNI Lasers) connected to the indwelling fibre optic by customized patch cords (BFL37-200 Custom; Thor Labs) and a double rotary joint (FRJ-1X2i; Doric Lenses) allowed mice to move freely during stimulation. The laser was triggered to deliver 4 ms pulses at 1 Hz or 13 Hz for 10 min, and the protocol was applied in the home cage 4 h before the first drug-seeking session or killing for *ex vivo* electrophysiology recordings. Mice from the control group were, in a randomized manner, either not infected with ChR2 or infected with eYFP only and received one of the optogenetic protocols, or were infected with ChR2 but were not exposed to light-stimulation. Seeking behaviour did not differ among these three control conditions, so the data were collapsed.

Test of cue-associated drug seeking. Thirty days after the final self-administration session (that is, day 40), mice were assigned to optogenetic protocol groups (control, 1 or 13 Hz) according to performance during self-administration acquisition, such that acquisition did not differ between the groups. Control animals were included for each batch of tested animals explaining the greater number of mice in the control group. The cue-associated drug-seeking test was a 60 min session, identical to the cocaine acquisition period (house light on, insertion of the two levers), except that one press on the active lever (FR1 schedule) now triggered illumination of the cue

light for 5 s but without a cocaine infusion or a timeout period. The infusion pump was also activated during the drug-seeking session, because the pump noise provided an extra drug-associated cue. One week later (that is, day 48), mice undertook a second drug-seeking session (with no further optogenetic stimulation 4 h before) to assess the persistence of the optogenetic protocol on seeking behaviour. At the end of any behavioural experiment, mice were euthanized and brains fixed in paraformaldehyde to prepare histological slices for verification of Chr2 expression and cannula placement (see Extended Data Fig. 9).

Food training after drug seeking. Immediately after the second drug-seeking test, subgroups of mice were food deprived for 12 h and then started nine consecutive sessions of operant training for food to examine whether optogenetic protocols had long-term effects on the acquisition of new learning for a natural reward. The test was performed in similar chambers as used previously (ENV-307A-CT, Med Associates), except that two nose-poke holes were present instead of levers at each side of a food pellet dispenser. One nose-poke in the active hole (randomly assigned) illuminated the cue light for 5 s and triggered the delivery of one food pellet (50% sucrose, AIN-76A Rodent Tablet 20 mg, Testdiet). The response requirement was set at FR1 for sessions 1–3, FR2 for sessions 4–6 and FR3 for sessions 7–9. The house light was turned off during the entire session. Each session ended after 30 min or when 45 pellets had been delivered, whichever occurred first. Each mouse received 2.7–3 g per day of standard laboratory chow during the food training procedure to maintain a stable body weight without any further weight gain.

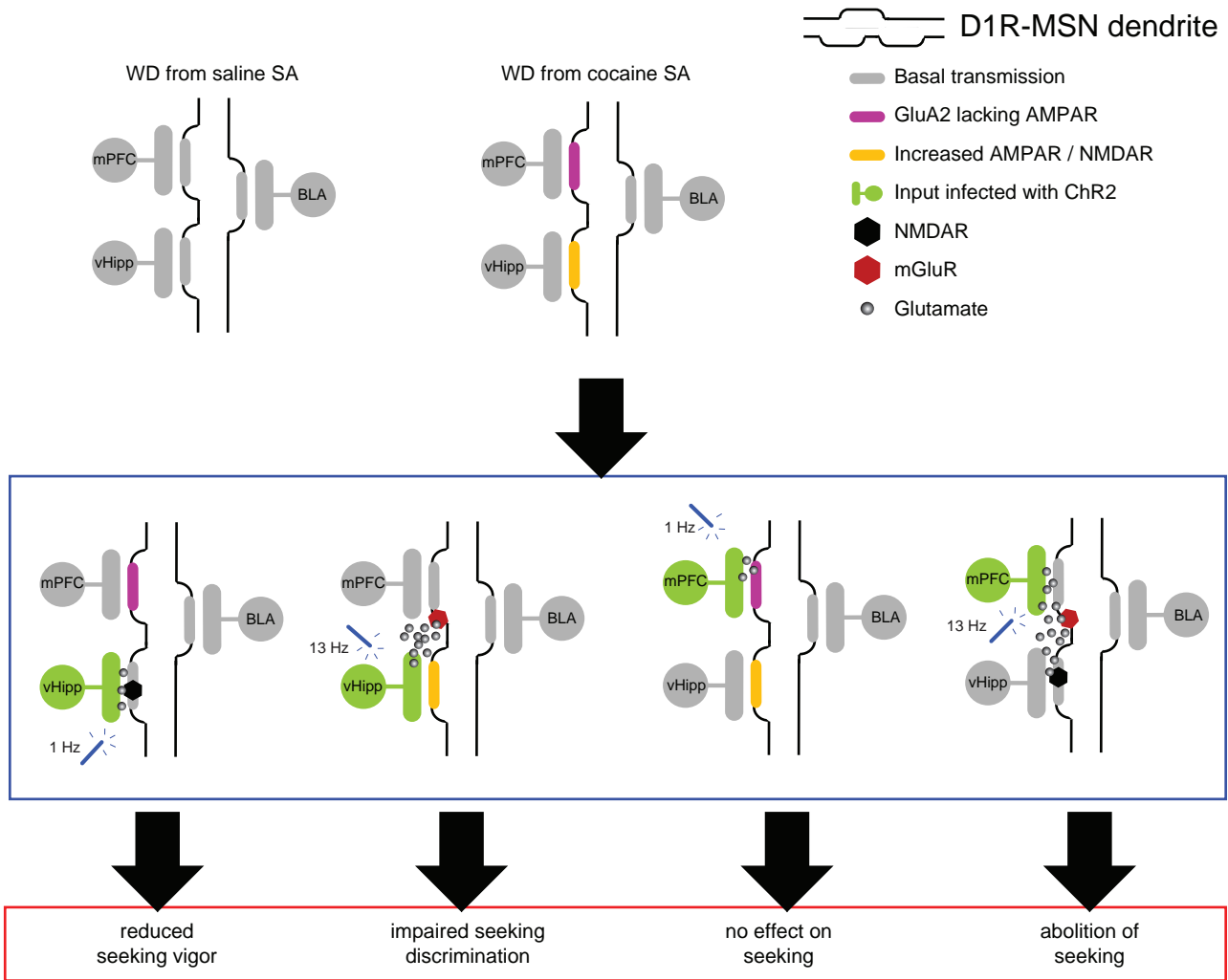
Effect of optogenetic protocols on cue-associated food seeking. To assess the specificity of the optogenetic treatment for drug versus food cue-associated seeking, we also tested a new cohort of mice for cue-associated food seeking after the optogenetic protocol. Mice underwent food training in the same conditions as for the cocaine self-administration group except that cocaine infusions were replaced by sucrose pellet delivery. Sessions ended after 30 min or when 45 pellets were delivered, whichever occurred first. After implantation of fibre optic cannula at day 15–20 of forced abstinence from sucrose pellet consumption, mice were assigned to the control or 13 Hz groups (such that acquisition did not differ between the groups) and received the optogenetic treatment 4 h before a test for food-reward seeking that was undertaken in the same way as the test for cocaine seeking. The sound of the pellet dispenser was also paired with the food cue light during the session. Food seeking sessions lasted 30 min. Mice received 2.7–3 g per day of standard laboratory chow over the entire procedure to maintain a stable body weight (no weight gain).

Slice electrophysiology. Coronal 200–250 μm slices of mouse brain were prepared in cooled artificial cerebrospinal fluid containing (in mM): NaCl 119, KCl 2.5, MgCl 1.3, CaCl₂ 2.5, Na₂HPO₄ 1.0, NaHCO₃ 26.2 and glucose 11, bubbled with 95% O₂ and 5% CO₂. Slices were kept at 32–34 °C in a recording chamber superfused with 2.5 ml min⁻¹ artificial cerebrospinal fluid. Visualized whole-cell voltage-clamp recording techniques were used to measure holding and synaptic responses of MSNs of the NAc shell, identified by the presence of the eGFP or td-Tomato of BAC transgenic mice by using a fluorescent microscope (Olympus BX50WI, fluorescent light U-RFL-T). Note that when using Chr2-eYFP in BAC transgenic mice, D2R-MSNs were identified as D2R-eGFP-positive neurons in Drd2-eGFP mice, which could be visualized against fluorescence from Chr2-eYFP, or as tomato-negative neurons in Drd1a-tdTomato mice. D1R-MSNs were always identified as tomato-positive cells. This approach was validated in a previous report (ref. 28). The holding potential was -70 mV, and the access resistance was monitored by a hyperpolarizing step of -14 mV with each sweep, every 10 s. The liquid junction potential was small (-3 mV), and therefore traces were not corrected. Experiments were discarded if the access resistance varied by more than 20%. Currents were amplified (Multiclamp 700B, Axon Instruments), filtered at 5 kHz and digitized at 20 kHz (National Instruments Board PCI-MIO-16E4, Igor, WaveMetrics). All experiments were performed in the presence of picrotoxin (100 μM).

For recordings of light- and electrically evoked EPSCs, the internal solution contained (in mM) 130 CsCl, 4 NaCl, 5 creatine phosphate, 2 MgCl₂, 2 Na₂ATP, 0.6 Na₃GTP, 1.1 EGTA, 5 HEPES and 0.1 mM spermine. In some cases, QX-314 (5 mM) was added to the solution to prevent action currents. Synaptic currents were electrically evoked by stimuli (50–100 μs) at 0.1 Hz through bipolar stainless steel electrode placed onto the tissue. For optogenetic experiments, light-EPSCs were evoked with 4 ms blue light pulses from an optic fibre directed at the NAc shell that was coupled to a DPSS blue light laser. Low-frequency stimulation (1 or 13 Hz for 10 min) was applied with 4 ms light pulses and the magnitude of LTD was determined by comparing average EPSCs that were recorded 20–30 min after induction to EPSCs recorded immediately before induction. To isolate AMPAR-evoked EPSCs, the NMDA antagonist D-AP5 (50 μM) was bath applied. The NMDAR component was calculated as the difference between the EPSCs measured in the absence and in the presence of D-AP5. The AMPAR/NMDAR ratio was calculated by dividing the peak amplitudes. The rectification index of AMPAR was calculated as the ratio of the chord conductance calculated at negative potential divided by chord conductance at positive potential. Note that, in example traces, stimulation artefacts were removed.

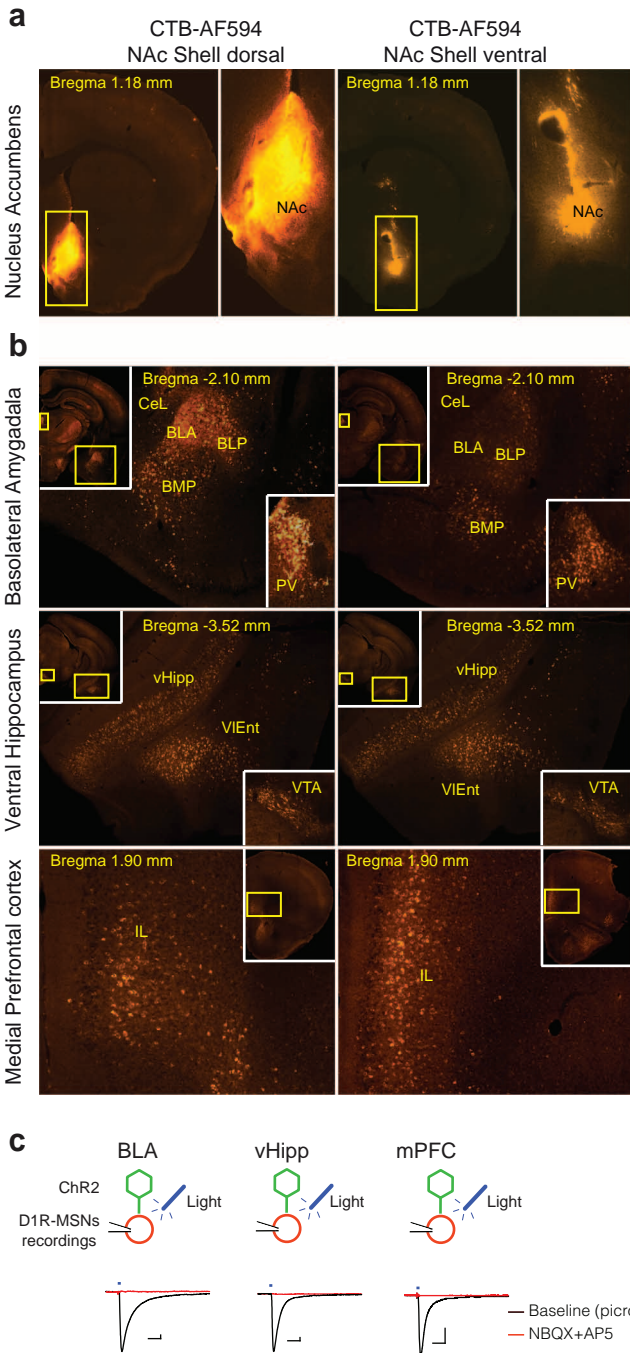
For recordings of mEPSCs the internal solution contained (in mM): 140 K Glu, 2 MgCl₂, 5 KCl, 0.2 EGTA, 10 HEPES, 4 Na₂ATP, 0.3 Na₃GTP and 10 creatine phosphate. Miniature EPSCs were recorded in the presence of tetrodotoxin (0.5 μM). The frequencies, amplitudes and kinetic properties of these currents were then analysed using the Mini Analysis software package (version 4.3, Synaptosoft). Note that recordings were performed with the electrophysiologist blinded to the self-administration condition (cocaine or saline), although for practical reasons the experimenter was aware of other conditions (for example, Chr2 infected or not, etc.). **Statistics.** No statistics were used to determine group sample size; however, sample sizes were similar to those used in previous publications from our group and others reporting self-administration in mice. Multiple comparisons were first subject to mixed-factor ANOVA defining both between- (for example, D1R- or D2R-MSN cells; saline or cocaine self-administration groups; control, 1 Hz or 13 Hz protocols; BLA, vHIP, mPFC inputs, etc.) and/or within- (for example, active or inactive levers) group factors. Where significant main effects or interaction terms were found ($P \leq 0.05$; or $P \leq 0.1$ indicative of a trend), further comparisons were made by a two-tailed Student's *t*-test with Bonferroni corrections applied when appropriate (that is, the level of significance equalled 0.05 divided by the number of comparisons). Single comparisons of between- or within-group measures were made by two-tailed non-paired or paired Student's *t*-test, respectively. ANOVAs for main figures are provided (see Extended Data Table 1a, b)

44. Franklin, K. B. J. & Paxinos, G. *The Mouse Brain in Stereotaxic Coordinates* 3rd edn (Elsevier Academic Press, 2008).
45. Bertran-Gonzalez, J. *et al.* Opposing patterns of signaling activation in dopamine D1 and D2 receptor-expressing striatal neurons in response to cocaine and haloperidol. *J. Neurosci.* **28**, 5671–5685 (2008).
46. Ouimet, C. C. *et al.* DARPP-32, a dopamine- and adenosine 3':5'-monophosphate-regulated phosphoprotein enriched in dopamine-innervated brain regions. III. Immunocytochemical localization. *J. Neurosci.* **4**, 111–124 (1984).
47. Thomsen, M. & Caine, S. B. Intravenous drug self-administration in mice: practical considerations. *Behav. Genet.* **37**, 101–118 (2006).
48. Chistyakov, V. S. & Tsibulsky, V. L. How to achieve chronic intravenous drug self-administration in mice. *J. Pharmacol. Toxicol. Methods* **53**, 117–127 (2006).
49. Gipson, C. D. *et al.* Relapse induced by cues predicting cocaine depends on rapid, transient synaptic potentiation. *Neuron* **77**, 867–872 (2013).
50. Sparta, D. R. *et al.* Construction of implantable optical fibers for long-term optogenetic manipulation of neural circuits. *Nature Protocols* **7**, 12–23 (2011).



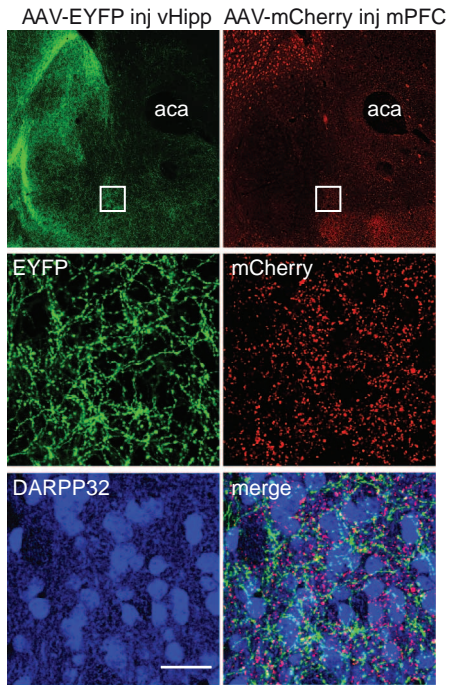
Extended Data Figure 1 | Graphical abstract. Top left: main excitatory afferents onto NAc shell D1R-MSNs (BLA: basolateral amygdala, vHipp: ventral subiculum of the hippocampus and mPFC: medial prefrontal cortex), which at baseline contain synapses that express NMDARs and GluA2-containing AMPARs. Top right: 1 month after withdrawal (WD) from cocaine self-administration (SA), mPFC synapses onto NAc shell D1R-MSNs express

GluA2-lacking AMPARs whereas more GluA2-containing AMPARs are added at vHipp synapses. Effects of NMDAR- or mGluR1-dependent (1 or 13 Hz, respectively) light protocols applied at specific inputs (shown in green) on cocaine-evoked plasticity are illustrated, together with the consequence for cue-associated seeking behaviour.

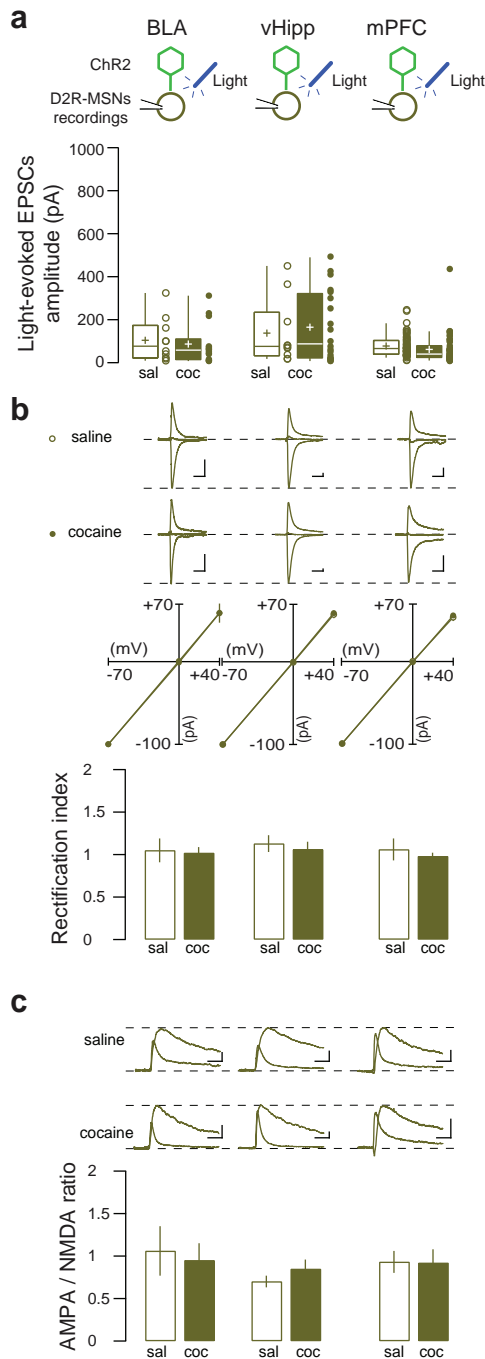


Extended Data Figure 2 | Identification and optogenetic targeting of excitatory inputs to the NAc shell. **a**, Retrograde labelling with cholera toxin subunit B (AF594) injected into the NAc shell. Confocal images of injection sites (top) in the medio-dorsal (left) and medio-ventral (right) NAc shell are shown, regions where electrophysiology recordings were performed.

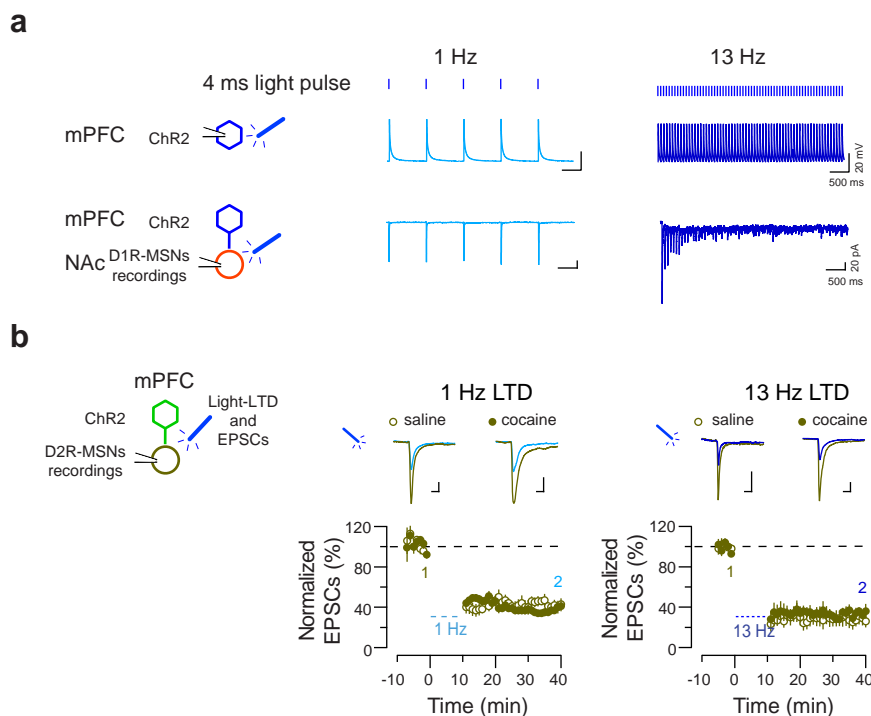
b, Labelled cell bodies in corresponding projection areas (basolateral amygdala, ventral subiculum of the hippocampus and medial prefrontal cortex) are shown, with no discernable segregation between the medio-dorsal or medio-ventral NAc shell. For each projection area, the insert shows a complete hemisphere coronal section together with a zoomed image of the region of interest (indicated by yellow box). IL, infralimbic; CeL; central amygdala lateral; BLP, basolateral amygdala posterior; BMP, basomedial amygdala posterior; PV, paraventricular thalamic nucleus; vHipp, central subiculum of the hippocampus; VIEnt, ventral intermediate entorhinal cortex; VTA, ventral tegmental area. **c**, Schematic of experiment (top) with light-evoked EPSCs recorded in D1R-MSNs of the NAc shell of mice infected with AAV1-ChR2-eYFP in the BLA (bottom left), vHipp (middle) or vmPFC (right) before and after bath application of glutamate receptor antagonists (NBQX 10 μ M and AP5 50 μ M for AMPAR and NMDAR, respectively). Scale bars, 20 ms, 50 pA.



Extended Data Figure 3 | Individual MSNs receive inputs from multiple projection areas. **a**, Confocal images of NAc from a mouse infected with AAV5-EF1-eYFP and AAV5-EF1-mCherry in the vHipp (left) and mPFC (right), respectively, at low magnification (first row). At higher magnification (second and third rows) eYFP from vHipp and mCherry from mPFC are present around MSNs stained by DARPP-32 (blue). aca, anterior commissure. Scale bar, 50 μ m.

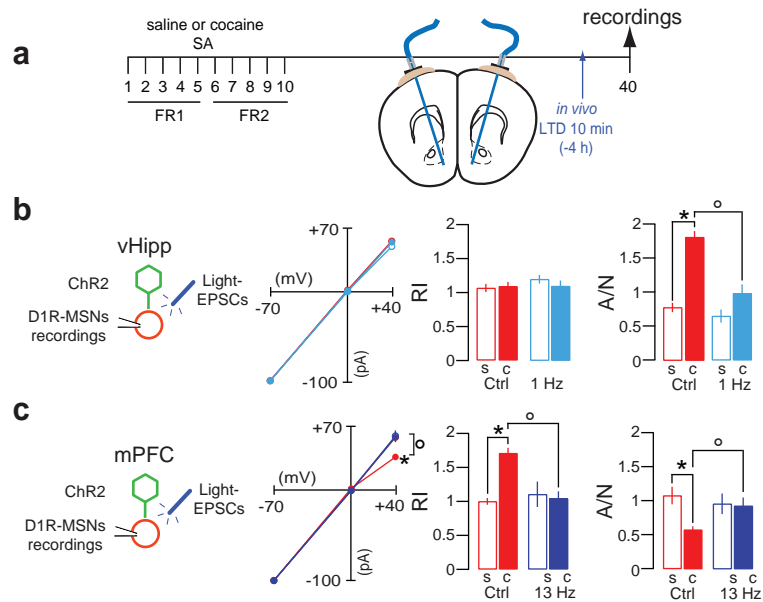


Extended Data Figure 4 | Cocaine self-administration does not evoke input-specific plasticity in D2R-MSNs. **a**, Top, schematic of whole-cell recordings of NAc shell D2R-MSNs of mice that 1 month previously self-administered saline (open points) or cocaine (filled points) and were infected with AAV1-ChR2-eYFP in the BLA (left), vHipp (middle) or mPFC (right). Bottom, after cocaine self-administration the mean amplitude of light-evoked EPSCs was not changed at any input onto D2R-MSNs (effect of group (saline/cocaine) and group \times input (BLA/vHipp/mPFC) all not significant) ($n = 10/14$ for BLA (saline/cocaine), $n = 10/20$ for vHipp and $n = 60/51$ for mPFC). **b**, For each input, the rectification index (RI) was calculated. Example traces are shown (top), with the I/V plot (middle) and group mean rectification index data (bottom). Cocaine did not modify normalized AMPAR-EPSCs at +40 mV from BLA, vHipp or mPFC inputs ($t_{12} = -0.20$, $P = 0.84$, $t_{18} = 0.44$, $P = 0.67$ and $t_{20} = 0.43$, $P = 0.67$, respectively). The rectification index was also unchanged at D2R-MSN synapses from BLA, vHipp or mPFC inputs ($t_{12} = -0.32$, $P = 0.75$, $t_{18} = -0.51$, $P = 0.62$ and $t_{20} = -0.67$, $P = 0.51$ respectively). Scale bars, 20 ms, 20 pA. **c**, For the same cells as shown in **b**, the A/N ratio was calculated. For each input, example traces are shown (top), with group mean A/N ratios (bottom). Cocaine did not alter the A/N ratio at inputs onto D2R-MSNs from the BLA, vHipp or mPFC ($t_{12} = -0.19$, $P = 0.85$, $t_{18} = 1.20$, $P = 0.25$ and $t_{20} = -0.04$, $P = 0.97$, respectively). Scale bars, 20 ms, 20 pA. Error bars, s.e.m.



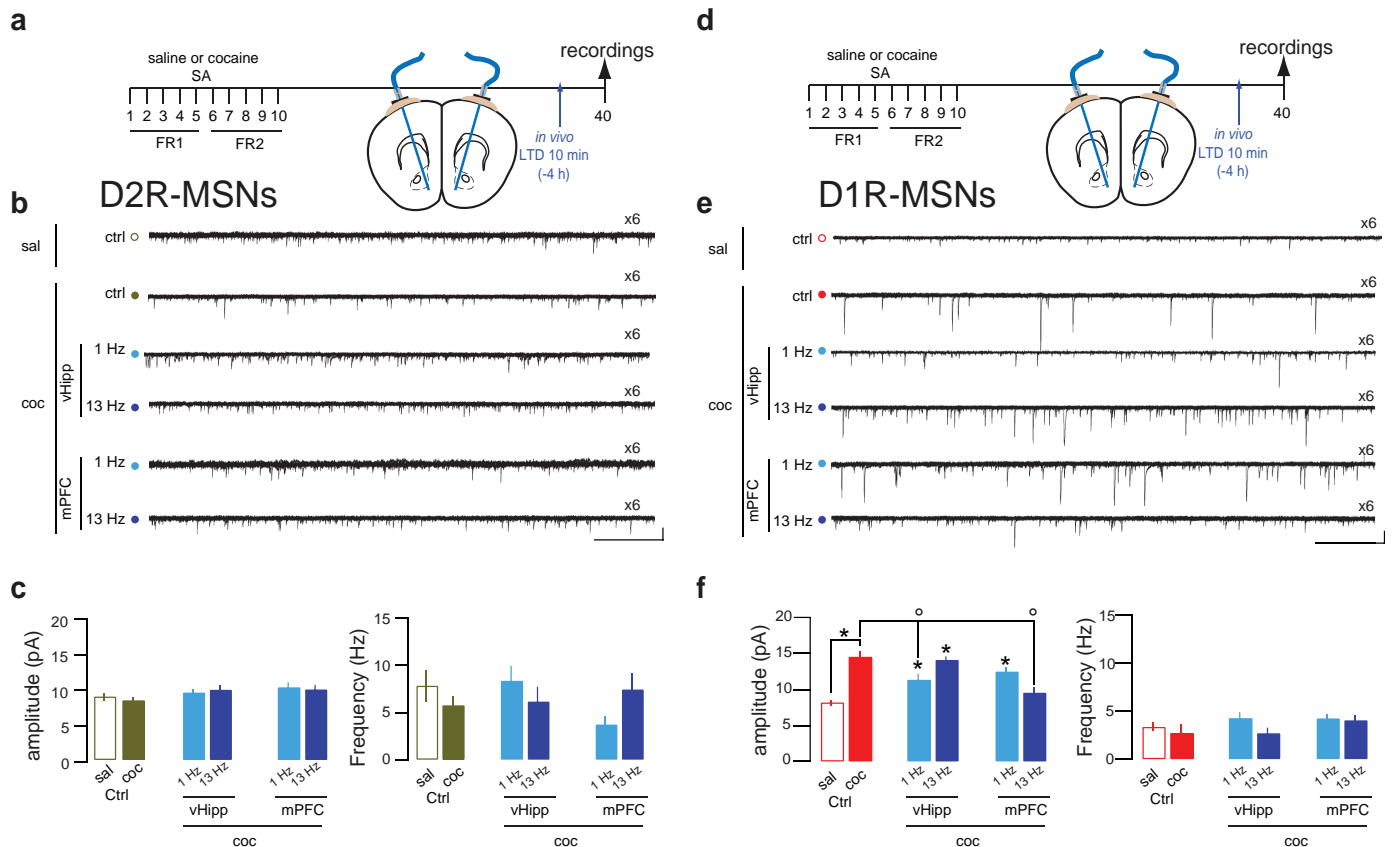
Extended Data Figure 5 | mPFC and NAc recordings during 1 and 13 Hz optogenetic protocols and LTD in NAc D2R-MSNs induced by mPFC protocols applied after saline and cocaine self-administration. **a**, Right, schematic of whole-cell recordings in the mPFC or NAc from mice infected with ChR2 in mPFC. Top, light-evoked action potentials recorded in current clamp of ChR2-infected mPFC neurons and EPSCs recorded in voltage-clamp of D1R-MSNs (bottom) during the beginning of the 1 Hz (left) or 13 Hz (right) stimulation protocols. Note that EPSCs fail to follow the 13 Hz protocol. **b**, Top left, schematic of experiment. Bottom, graph of normalized light-evoked

EPSCs across time recorded in NAc D2R-MSNs from saline and mice that self-administered cocaine (each point represents mean of six sweeps), together with example traces (mean of 20 sweeps) before (1) and after (2) a 1 (left) or 13 Hz (right) light protocol was applied *ex vivo* (4 ms pulses at 1 or 13 Hz, 10 min). One month after saline or cocaine self-administration, the 1 Hz and 13 Hz protocols induced comparable LTDs in both groups (for 1 Hz: $50 \pm 4.9\%$ to $40 \pm 2.6\%$, Student's t -test $t_{14} = -1.86$, $P = 0.080$; $n = 7-9$ cells; for 13 Hz: $28 \pm 3.7\%$ to $33 \pm 4.2\%$, Student's t -test $t_{18} = 1.41$, $P = 0.18$; $n = 11-9$ cells). Error bars, s.e.m.



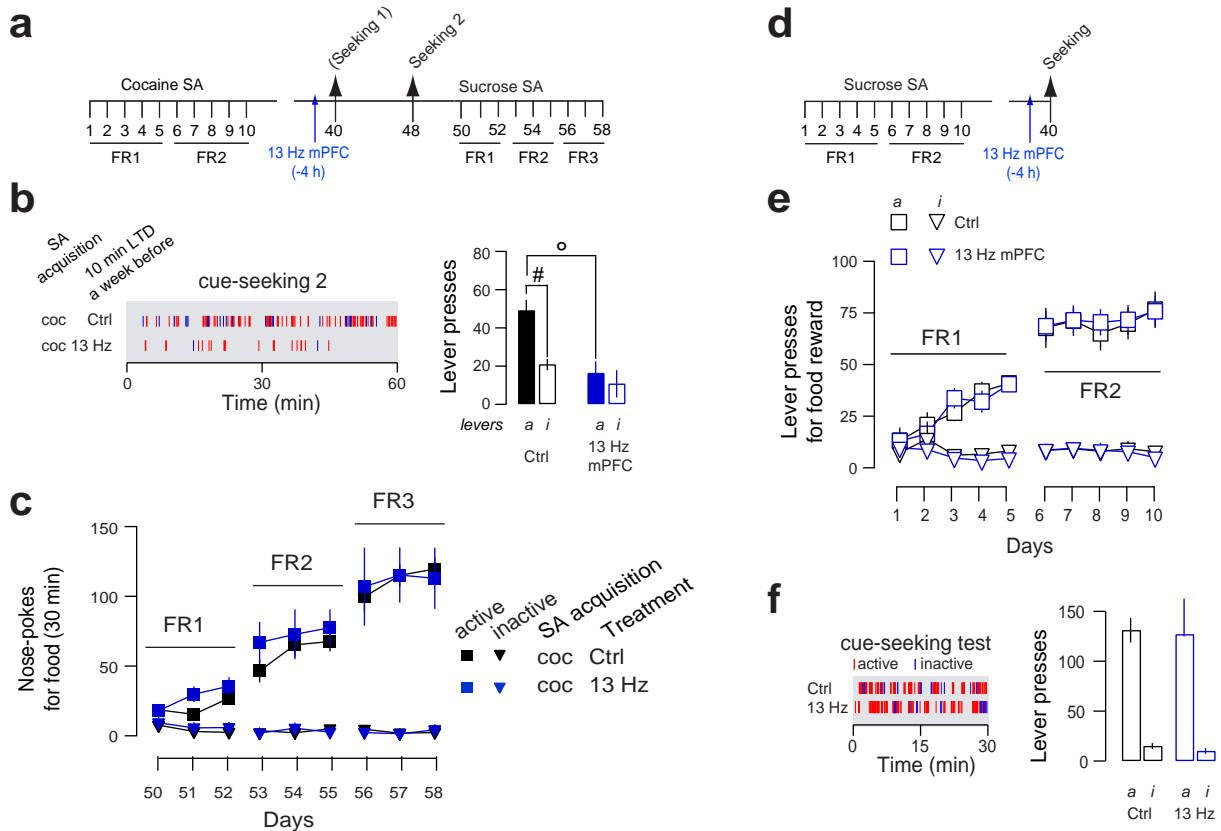
Extended Data Figure 6 | Optogenetic protocols applied *in vivo* reverse cocaine evoked-plasticity at NAc D1R-MSNs. **a**, Top, schematic of experiment. Mice were infected with ChR2 in the vHipp or mPFC and trained in saline or cocaine self-administration. Mice were then implanted with fibre optics targeting the NAc shell, and optogenetic protocols were applied *in vivo* 1 month after withdrawal. Four hours later, acute brain slices were prepared to assess the efficiency of optogenetic protocols applied *in vivo* to reverse cocaine-evoked plasticity at NAc D1R-MSNs. In brief, consistent with the *ex vivo* validation, the 1 Hz vHipp protocol applied *in vivo* normalized the *A/N* ratio, whereas the 13 Hz mPFC protocol normalized the *I/V* curve and rectification index in mice that self-administered cocaine. **b**, Left, schematic of experiment indicating that mice were infected with ChR2 in the vHipp. The rectification index and *A/N* ratio were determined with light-evoked EPSCs as described previously (see Fig. 2). The *I/V* plot is shown, together with group mean rectification index and *A/N* data. Cocaine did not alter normalized AMPAR-EPSCs recorded at +40 mV or the rectification index from vHipp inputs (same data as Fig. 3). The 1 Hz protocol applied *in vivo* was without effect on either of these measures in mice that self-administered saline or

cocaine (effect of group (saline versus cocaine), protocol (control versus 1 Hz) and group \times protocol, all not significant). The *A/N* ratio was increased at vHipp inputs in mice that self-administered cocaine (same data as Fig. 3), an effect that was reduced after the *in vivo* 1 Hz protocol (planned comparison, after ANOVA, by *t*-test, $t_{26} = 4.97$, $^{\circ}P < 0.001$) ($n = 13/15$ for 1 Hz saline/cocaine group). **c**, As for **b**, except that mice were infected with ChR2 in the mPFC. Cocaine decreased AMPAR-EPSCs recorded at +40 mV and increased the rectification index from mPFC inputs (same data as Fig. 3). The 13 Hz protocol applied *in vivo* increased AMPAR-EPSCs at +40 mV in mice that self-administered cocaine (planned comparison with cocaine control group, after ANOVA, by *t*-test, $t_{20} = 3.6$, $^{\circ}P < 0.01$) and decreased the rectification index in mice that self-administered cocaine (planned comparison with cocaine controls, after ANOVA, by *t*-test, $t_{20} = 5.2$, $^{\circ}P < 0.001$). The *A/N* ratio was decreased at mPFC inputs in mice that self-administered cocaine (same data as Fig. 3), an effect that was normalized after the *in vivo* 13 Hz protocol (planned comparison with cocaine controls, after ANOVA, by *t*-test, $t_{20} = 2.8$, $^{\circ}P = 0.01$) ($n = 11/9$ for 13 Hz saline/cocaine group). Error bars, s.e.m.



Extended Data Figure 7 | Assessing effects of *in vivo* light stimulation on mEPSCs recorded in D2R- and D1R-MSNs. **a**, Top, schematic of experiment. Mice were infected with Chr2 in the vHipp or mPFC and trained in saline or cocaine self-administration. Mice were then implanted with fibre optics targeting the NAc shell and optogenetic protocols applied *in vivo* 1 month after withdrawal. Four hours later, acute brain slices were prepared to assess the effect of optogenetic protocols applied *in vivo* on global excitatory transmission by recording mEPSCs at NAc D2R-MSNs. In brief, recordings from D2R-MSNs showed that mEPSCs were not affected by cocaine and not depressed by optogenetic LTD protocols applied *in vivo*. Note that although optogenetic protocols efficiently induced LTD at single inputs onto D2R-MSNs (Extended Data Fig. 5), this was not reflected by a decrease in mEPSC amplitudes. This may be accounted for by a presynaptic expression mechanism of LTD or that baseline amplitudes were already low such that a further depression only at a single input could not be measured by mEPSCs (that is, floor effect), which reflects synaptic transmission from multiple inputs. **b**, Example of mEPSCs recorded *ex vivo* in NAc shell D2R-MSNs in the presence of picrotoxin (100 μ M) and tetrodotoxin (0.5 μ M) (sample traces comprising six superimposed, 4 s traces). Scale bars, 20 pA, 500 ms. **c**, Histograms of group mean data of D2R-MSN mEPSC amplitudes (left) and frequency (right) are shown in control saline (sal) or cocaine (coc) conditions and after application of 1 Hz or 13 Hz light protocols at vHipp or mPFC synapses. Mean mEPSC amplitudes and frequencies were not changed by cocaine, and were not significantly decreased by protocols applied at either

vHipp or mPFC inputs ($n = 5$ to 13 cells per group). Error bars, s.e.m. **d**, **e**, As for **a** and **b** except in D1R-MSNs. In brief, the frequency of mEPSCs was not affected by cocaine self-administration or laser protocols. In contrast, in mice that self-administered cocaine the amplitude of mEPSCs was significantly larger than controls, in line with a postsynaptic expression mechanism. Protocols that were most efficient at restoring the A/N ratio at vHipp synapses when assessed on slice, namely the 13 Hz mPFC and the 1 Hz vHipp protocol, were also most efficient at restoring baseline mEPSC amplitudes when applied *in vivo*. This suggests that cocaine-evoked plasticity at vHipp inputs largely accounts for the observed increase in mEPSC amplitudes. **f**, Mean mEPSC amplitudes were increased by cocaine self-administration (versus saline control, by *t*-test, $t_{18} = 7.13$, $^*P < 0.001$). Protocols applied at vHipp terminals altered mEPSC amplitudes (one-way ANOVA comparing cocaine control, 1 and 13 Hz vHipp protocols: effect of protocol $F_{2,28} = 5.7$, $P < 0.01$). The 1 Hz but not the 13 Hz vHipp protocol reduced mEPSC amplitudes (versus cocaine control, for 1 Hz: $t_{18} = 2.8$, $^{\circ}P = 0.01$), although amplitudes remained significantly higher than saline control mice after either protocol (all $P < 0.01$). Protocols applied at mPFC terminals also altered mEPSC amplitudes (effect of protocol, $F_{2,29} = 13.1$, $P < 0.001$), and the 13 Hz but not 1 Hz mPFC protocol reduced mEPSC amplitudes (versus cocaine control, for 1 Hz: $t_{19} = 4.7$, $^{\circ}P < 0.001$). Moreover, amplitudes after the 13 Hz mPFC protocol did not differ from saline controls ($P = 0.14$). The frequencies of mEPSCs were not altered by cocaine or by protocols applied at either vHipp or mPFC inputs ($n = 8-11$ cells per group). All error bars, s.e.m.

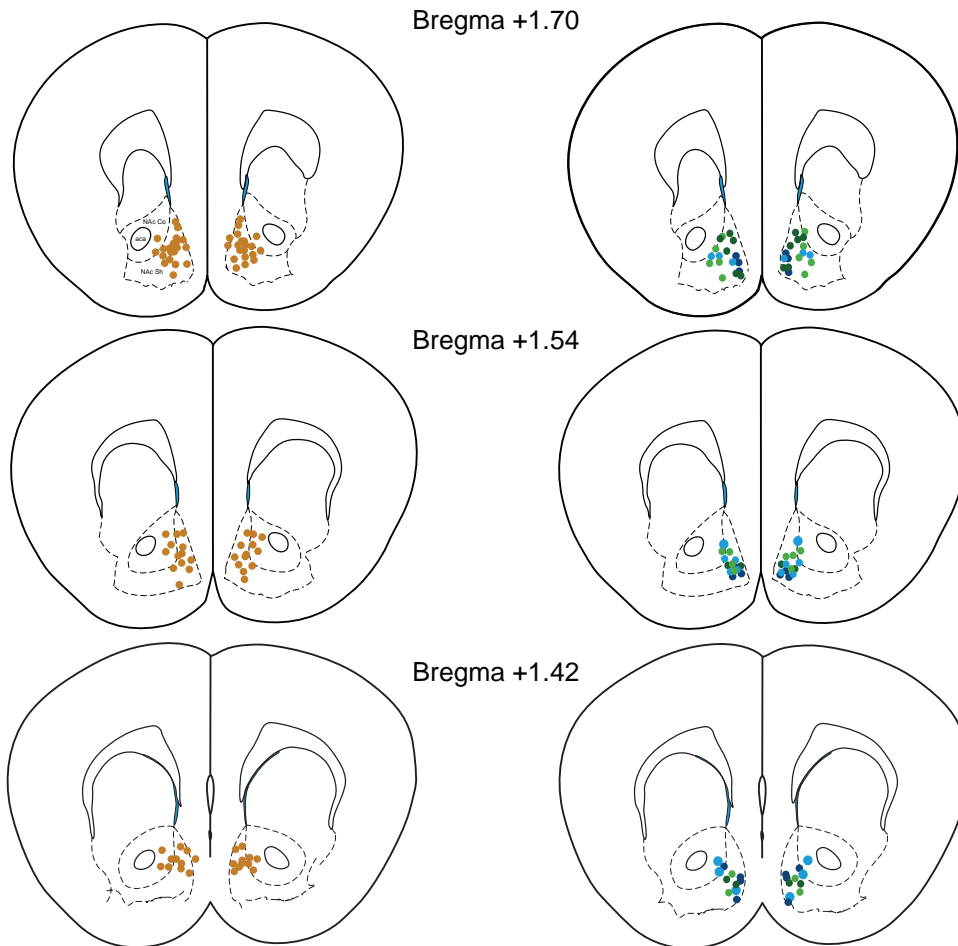


Extended Data Figure 8 | Optogenetic effect on cocaine seeking is persistent, and does not alter learning of a new response for food reward or food cue-associated seeking. **a**, Schematic of experiment. Cocaine control and 13 Hz mPFC group mice were exposed to a second cocaine cue-associated seeking test 1 week after the first test (see Fig. 5), but without further optogenetic intervention. Two days after this second test, subgroups of mice from each condition were trained to nose-poke for sucrose pellets during once-daily 30 min sessions over 9 days. **b**, Raster plots of cue-associated seeking behaviour (active and inactive lever presses) during the second test are shown (left), together with group mean data showing active (a: filled boxes) and inactive (i: open boxes) lever presses. Seeking was present in cocaine control mice during the second test, but was absent in the 13 Hz mPFC group (effect of group, group and lever group, all $P < 0.05$; active versus inactive lever comparison by t -test, $t_{43} = 6.13$, $^{\#}P < 0.001$ for controls $n = 44$ and $t_9 = 0.97$, $P = 0.35$ for 13 Hz mPFC, $n = 10$; active versus active lever comparison, $^{\circ}P < 0.01$). **c**, For the acquisition of a new response test, group mean values are shown of active and inactive nose-pokes across training days. Responding was

maintained by FR1, FR2 and FR3 schedules. ANOVA comparisons of nose-poke responding across 3 days at each fixed ratio schedule confirmed no difference between cocaine self-administration control ($n = 15$) and 13 Hz mPFC ($n = 4$) mice (effects of group and day \times group \times nose poke interactions, all not significant). **d**, Schematic of experiment. One month after food self-administration training, mice received the 13 Hz mPFC light protocol, 4 h before a 30 min test of seeking. **e**, Graph shows mean of active (a) and inactive (i) lever presses for sucrose pellets by new cohort of mice ($n = 14$) infected or not with ChR2 in the mPFC. Training parameters were identical to those used for the acquisition of cocaine self-administration, except that sessions lasted only 30 min. **f**, Raster plots of active and inactive lever presses during a cue-associated sucrose seeking session (left), together with group mean data of total active (a) and inactive (i) lever presses during the 30 min seeking test. Food seeking was robust in control mice and did not differ in the 13 Hz mPFC group (effect of lever, $F_{1,12} = 163.7$, $P < 0.002$; group and lever \times group all non-significant; $n = 6/8$). Error bars, s.e.m.

Tip of fibers in:

- control mice
- 13 Hz vHipp
- 1 Hz vHipp
- 1 Hz mPFC
- 13 Hz mPFC



Extended Data Figure 9 | Position of fibre optic cannula placements for mice used in tests of cue-seeking. Figure shows identified fibre optic cannula tip placements in controls (left) or mice that received different light protocols

targeting either vHipp or mPFC to NAc synapses (right). Note that when mice were used for electrophysiology recordings, fibre optic placements were visually confirmed but not recorded.

Extended Data Table 1 | ANOVA comparisons for (a) Figs 1–4 and (b) Fig. 5

a

| Figure | Measure | ANOVA factors | Effect | F | P |
|------------|---|---|------------------|----------------|--------|
| 1c | RI | Cell (D1R-MSN, D2R-MSN) x Group (saline, cocaine) | Group | F(1,83)=10.86 | 0.001 |
| | | | Cell | F(1,83)=3.18 | <0.1 |
| | | | Group x Cell | F(1,83)=6.08 | <0.05 |
| | A/N | Cell (D1R-MSN, D2R-MSN) x Group (saline, cocaine) | Group | F(1,83)=5.91 | <0.05 |
| | | | Cell | F(1,83)=11.91 | 0.001 |
| | | | Group x Cell | F(1,83)=8.34 | <0.01 |
| 2b | Amplitudes | Group (saline, cocaine) x Input (BLA, vHipp, mPFC) | Group | F(1,206)=6.44 | <0.05 |
| | | | Input | F(2,206)=18.01 | <0.001 |
| | | | Group x Input | F(2,206)=4.14 | <0.05 |
| 2c | RI | Group (saline, cocaine) x Input (BLA, vHipp, mPFC) | Group | F(1,56)=14.56 | <0.001 |
| | | | Input | F(2,56)=9.87 | <0.001 |
| | | | Group x Input | F(2,56)=18.03 | <0.001 |
| 2d | A/N | Group (saline, cocaine) x Input (BLA, vHipp, mPFC) | Group | F(1,56)=1.64 | n.s. |
| | | | Input | F(2,56)=11.44 | <0.001 |
| | | | Group x Input | F(2,56)=33.41 | <0.001 |
| 3d | Amplitude @ +40 mV (vHipp) | Group (saline, cocaine) x Protocol (Control, 1 Hz, 13Hz) | Group | F(1,45)=0.32 | n.s. |
| | | | Protocol | F(2,45)=0.37 | n.s. |
| | | | Group x Protocol | F(2,45)=0.23 | n.s. |
| | RI (vHipp) | Group (saline, cocaine) x Protocol (Control, 1 Hz, 13Hz) | Group | F(1,45)=1.39 | n.s. |
| | | | Protocol | F(2,45)=0.64 | n.s. |
| | | | Group x Protocol | F(2,45)=0.78 | n.s. |
| 3e | A/N (vHipp) | Group (saline, cocaine) x Protocol (Control, 1 Hz, 13Hz) | Group | F(1,46)=59.43 | <0.001 |
| | | | Protocol | F(2,46)=9.76 | <0.001 |
| | | | Group x Protocol | F(2,46)=5.73 | <0.01 |
| 3i | Amplitude @ +40 mV (mPFC) | Group (saline, cocaine) x Protocol (Control, 1 Hz, 13Hz) | Group | F(1,54)=15.72 | <0.001 |
| | | | Protocol | F(2,54)=3.5 | <0.05 |
| | | | Group x Protocol | F(2,54)=2.57 | <0.1 |
| | RI (mPFC) | Group (saline, cocaine) x Protocol (Control, 1 Hz, 13Hz) | Group | F(1,54)=33.23 | <0.001 |
| | | | Protocol | F(2,54)=13.18 | <0.001 |
| | | | Group x Protocol | F(2,54)=10.72 | <0.001 |
| 3j | A/N (mPFC) | Group (saline, cocaine) x Protocol (Control, 1 Hz, 13Hz) | Group | F(1,54)=3.08 | <0.1 |
| | | | Protocol | F(2,54)=5.6 | <0.01 |
| | | | Group x Protocol | F(2,54)=6.0 | <0.01 |
| 4b | Amplitude @ +40 mV (vHipp) | Group (saline, cocaine) x Protocol (Control, 1 Hz, 13Hz) | Group | F(1,80)=9.92 | <0.05 |
| | | | Protocol | F(2,80)=3.37 | <0.05 |
| | | | Group x Protocol | F(2,80)=3.15 | <0.05 |
| RI (vHipp) | Group (saline, cocaine) x Protocol (Control, 1 Hz, 13Hz) | Group | F(1,80)=11.8 | 0.001 | |
| | | Protocol | F(2,80)=3.04 | 0.05 | |
| | | Group x Protocol | F(2,80)=3.39 | <0.05 | |
| 4c | A/N (vHipp) | Group (saline, cocaine) x Protocol (Control, 1 Hz, 13Hz) | Group | F(1,80)=13.5 | <0.001 |
| | | | Protocol | F(2,80)=5.6 | <0.01 |
| | | | Group x Protocol | F(2,80)=2.07 | n.s. |
| 4b | Amplitude @ +40 mV (mPFC) | Group (saline, cocaine) x Protocol (control, 1 Hz, 13 Hz) | Group | F(1,94)=12.1 | 0.001 |
| | | | Protocol | F(2,94)=0.6 | n.s. |
| | | | Group x Protocol | F(2,94)=3.96 | <0.05 |
| RI (mPFC) | Group (saline, cocaine) x Protocol (control, 1 Hz, 13 Hz) | Group | F(1,94)=16.95 | <0.001 | |
| | | Protocol | F(2,94)=2.3 | 0.1 | |
| | | Group x Protocol | F(2,94)=4.83 | 0.01 | |
| 4c | A/N (mPFC) | Group (saline, cocaine) x Protocol (control, 1 Hz, 13 Hz) | Group | F(1,94)=9.12 | <0.01 |
| | | | Protocol | F(2,94)=2.2 | n.s. |
| | | | Group x Protocol | F(2,94)=2.65 | <0.1 |

b

| Figure | Measure | Comparisons (ANOVA or t-test) | Effect | F | P |
|--|--|--|------------------|---------------|--------|
| 5b | Cocaine control vs. Saline control | Group (saline, cocaine) x Lever (active x inactive) | Lever | F(1,53)=21.7 | <0.001 |
| | | | Group | F(1,53)=16.8 | <0.001 |
| | | | Lever x Group | F(1,53)=22.9 | <0.001 |
| | Saline control | active vs. inactive | t(10)=0.43 | n.s. | |
| | | | t(43)=9.5 | <0.001 | |
| | Cocaine control | active vs. inactive | t(53)=4.6 | <0.001 | |
| | | | t(53)=4.6 | <0.001 | |
| | Cocaine control vs. Saline control | inactive lever comparison | t(53)=1.54 | n.s. | |
| | | | t(53)=1.54 | n.s. | |
| | 1 Hz vHipp vs. cocaine control | Lever (active, inactive) x Protocol (Control, Laser) | Lever | F(1,53)=45.7 | <0.001 |
| | | | Protocol | F(1,53)=4.7 | <0.05 |
| | | | Lever x Protocol | F(1,53)=5.13 | <0.05 |
| 1 Hz vHipp | active vs. inactive | t(10)=3.6 | <0.01 | | |
| | | t(53)=2.3 | <0.05 | | |
| 1 Hz vHipp vs. cocaine control | active lever comparison | t(53)=1.1 | n.s. | | |
| | | t(53)=1.1 | n.s. | | |
| 13 Hz vHipp vs. cocaine control | Lever (active, inactive) x Protocol (Control, Laser) | Lever | F(1,51)=30.8 | <0.001 | |
| | | Protocol | F(1,51)=4.12 | <0.05 | |
| | | Lever x protocol | F(1,51)=6.41 | <0.05 | |
| 13 Hz vHipp | active vs. inactive | t(8)=1.99 | n.s. | | |
| | | t(51)=0.39 | n.s. | | |
| 13 Hz vHipp vs. cocaine control | inactive lever comparison | t(51)=4.48 | <0.001 | | |
| | | t(51)=4.48 | <0.001 | | |
| 1 Hz mPFC vs. cocaine control | Lever (active, inactive) x Protocol (Control, Laser) | Lever | F(1,53)=52.08 | <0.001 | |
| | | Protocol | F(1,53)=1.1 | n.s. | |
| | | Lever x protocol | F(1,53)=3.08 | n.s. | |
| 1 Hz mPFC | active vs. inactive | t(10)=4.16 | 0.002 | | |
| | | t(10)=4.16 | 0.002 | | |
| 13 Hz mPFC vs. cocaine control | Lever (active, inactive) x Protocol (Control, Laser) | Lever | F(1,52)=23.2 | <0.001 | |
| | | Protocol | F(1,52)=16.7 | <0.001 | |
| | | Lever x protocol | F(1,52)=17.5 | <0.001 | |
| 13 Hz mPFC | active vs. inactive | t(9)=1.74 | n.s. | | |
| | | t(52)=4.29 | <0.001 | | |
| 13 Hz mPFC vs. cocaine control | inactive lever comparison | t(52)=2.19 | <0.05 | | |
| | | t(52)=2.19 | <0.05 | | |
| 5d | 13 Hz mPFC vs. food control | Lever (active, inactive) x Protocol (Control, Laser) | Lever | F(1,12)=163.7 | <0.001 |
| | | | Protocol | F(1,12)=0.022 | n.s. |
| | | | Lever x protocol | F(1,12)=0.41 | n.s. |